

# Targeted Delivery of Betulinic Acid to Cancer Cell Mitochondria by Using Gold Nanoparticles



Saima Asghar

Department of Physics  
School of Natural Sciences  
National University of Sciences and Technology, Islamabad,  
Pakistan

# Targeted Delivery of Betulinic Acid to Cancer Cell Mitochondria by Using Gold Nanoparticles



Saima Asghar

Regn. No.: 365305

**This work is submitted as a MS thesis in partial fulfillment of the requirement  
for the degree of  
(MS in Physics)**

**Dr Faheem Amin**

**Department of Physics**

**School of Natural Sciences (SNS)**

**National University of Sciences and Technology (NUST), H-12**

**Islamabad, Pakistan**

**Year 2023**

## THESIS ACCEPTANCE CERTIFICATE

Certified that final copy of MS thesis written by **Saima Asghar** (Registration No. **00000365305**), of **School of Natural Sciences** has been vetted by undersigned, found complete in all respects as per NUST statutes/regulations, is free of plagiarism, errors, and mistakes and is accepted as partial fulfillment for award of MS/M.Phil degree. It is further certified that necessary amendments as pointed out by GEC members and external examiner of the scholar have also been incorporated in the said thesis.

Signature: \_\_\_\_\_

Name of Supervisor: Dr. Faheem Amin

Date: 21-12-23

Signature (HoD): \_\_\_\_\_

Date: 21-12-2023

Signature (Dean/Principal): \_\_\_\_\_

Date: 21.12.2023

# National University of Sciences & Technology

## MS THESIS WORK

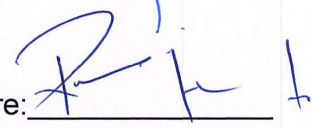
We hereby recommend that the dissertation prepared under our supervision by: Saima Asghar, Regn No. 00000365305 Titled: Targeted delivery of Betulinic Acid to Cancer Cell Mitochondria by Using Gold Nanoparticles be Accepted in partial fulfillment of the requirements for the award of **MS** degree.

### Examination Committee Members


1. Name: PROF. MUDASSIR IQBAL


Signature: 

2. Name: DR. RUMEZA HANIF

Signature: 

Supervisor's Name DR. FAHEEM AMIN

Signature: 

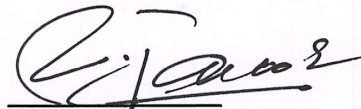
Co-Supervisor's Name PROF. SYED RIZWAN HUSSAIN Signature: 

  
Head of Department

21-12-2023  
 Date

### COUNTERSIGNED

Date: 21.12.2023

  
Dean/Principal

*I Dedicated this research work to my parents,  
Muhammad Asghar and Nasreen Asghar*

*For their endless love, support, and  
encouragement.*

## ***ACKNOWLEDGEMENT***

First and foremost, all my gratitude is for Allah almighty for blessing me with the opportunity to accomplish this task of submitting the MS thesis. I would like to thank my supervisors Professor **Dr. Faheem Amin** for their guidance, valuable advice, and motivation throughout the course of this work.

I am very thankful to the school administration for providing us with resources and sound environment for research. I am especially thankful to **Prof Rashid Farooq** principal SNS, and head of department and my GC member **Prof Dr Syed Rizwan** for their support. I am very grateful to my GC members **Dr Mudassir Iqbal** and **Dr Rumeza Hanif** for their valuable advice and suggestions.

I would like to acknowledge the effort and guidance of my seniors **Yasir Iqbal** and **Habiba Anjum**. I would also like to express my gratitude to all my friends, especially **Aamen Nasir, Sonadia, Khadija Javed Khan, Atiqa Amjad, Arooma Syed** and **Muqqadas** for their support and motivation.

I am utterly grateful to all my teachers. Finally, all my appreciation is toward my family, my parents, my brother **Mubashir Hassan** and my sisters **Ammara Asghar** And **Ayesha Asghar** for their love and support.

## **Abstract**

Globally, cancer is the biggest cause of mortality. Currently, breast cancer ranks fifth in terms of cancer-related mortality and is one of the most often diagnosed cancers. Conventional therapies have their limits. Drug delivery systems and many other approaches have been developed to address challenges such as hormone therapy, stem cell therapies, micelles, and nanoparticles. Specifically, nanoparticles engineered with multiple functionalities stand out as a promising solution to overcome various barriers associated with targeted delivery. Gold nanoparticles with a diameter of around 4 nm were synthesized using a two-phase method. The nanoparticle surface was subsequently modified with Polyethylene Glycol (PEG) to facilitate the loading of the hydrophobic drug Betulinic Acid. UV visible spectroscopy, Raman spectroscopy and FTIR analysis confirm the surface modification. We introduce these nanoparticles into the mitochondria of cancerous cells and initiate apoptosis. The outcomes of the MTT assay revealed that gold nanoparticles, modified with Polyethylene Glycol (PEG) and loaded with Betulinic Acid (BA), exhibited greater toxicity toward MDA-MB-231 cells as compared to HEK-293 cells. The modification of gold nanoparticles enhanced the suppressive impact of BA on MDA-MB-231 cells, primarily attributed to increased accumulation of reactive oxygen species (ROS) and caused change in mitochondrial membrane potential (MMP).

**Keywords:** *Gold Nanoparticles, Breast Cancer, Apoptosis, Targeted Drug Delivery, Mitochondrial Membrane potential (MMP), Betulinic Acid*

## ***Table of Contents***

|   |                  |
|---|------------------|
| <b><i>Introduction</i></b> .....                              | <b><i>1</i></b>  |
| 1.1 What is Cancer? .....                                     | 1                |
| 1.2 Types of Cancer .....                                     | 2                |
| 1.3 Main Causes of Cancers.....                               | 3                |
| 1.4 Breast Cancer .....                                       | 4                |
| 1.5 Traditional Methods of Cancer Treatment .....             | 5                |
| 1.6 Nanoparticles and Nanomedicine .....                      | 6                |
| 1.7 Gold Nanoparticles .....                                  | 11               |
| 1.9 Betulinic acid .....                                      | 20               |
| <b><i>Chapter 2</i></b> .....                                 | <b><i>22</i></b> |
| <b><i>Literature review</i></b> .....                         | <b><i>22</i></b> |
| <b><i>Chapter 3</i></b> .....                                 | <b><i>26</i></b> |
| <b><i>Apparatus and characterization techniques</i></b> ..... | <b><i>26</i></b> |
| 3.1 Apparatus .....   | 26               |
| 3.2 Characterization Technique .....                          | 28               |
| 4.2 Method .....  | 37               |
| <b><i>Chapter 5</i></b> .....                                 | <b><i>44</i></b> |
| <b><i>Result and Discussion</i></b> .....                     | <b><i>44</i></b> |
| UV Vis spectroscopy of Gold Nanoparticles .....               | 44               |
| FTIR Spectra of Gold Nanoparticles .....                      | 45               |
| RAMAN of Gold Nanoparticles .....                             | 46               |
| X-Ray Diffraction .....                                       | 47               |
| Gel electrophoresis.....                                      | 49               |
| Zeta Potential .....  | 50               |
| Cytotoxicity.....   | 53               |
| <b><i>Conclusion</i></b> .....                                | <b><i>57</i></b> |
| <b><i>Future Recommendations</i></b> .....                    | <b><i>58</i></b> |



## Table of Figures

|  |    |
|--|----|
| Figure 1: GLOBOCAN 2020 Statistic. [2] .....   | 1  |
| Figure 2: Anatomical diagram of the normal breast (mammary gland) showing the structure of glandular tissues, lobules and stromal tissue within the breast mound. [6] .....  | 5  |
| Figure 3: Systematical diagram of traditional methods for cancer treatment [8] .....   | 6  |
| Figure 4: Generation of Drug Delivery System. [9].....   | 9  |
| Figure 5: Different Advantages of Using Gold Nanoparticles .[21] .....   | 12 |
| Figure 6: The interaction of electromagnetic radiation with the metal sphere causes the formation of surface plasmons in metallic nanoparticles. A dipole is created, which oscillates in phase with the incoming light's electric field.[24].....   | 14 |
| Figure 7: Different steps of apoptosis. Start with cellular shrinkage than membrane oligomerization and nucleus collapse at the end apoptotic bodies form which are eventually engulfed by macrophages. [30]   | 16 |
| Figure 8: Structure of Mitochondria [31]. .....  | 17 |
| Figure 9: Intrinsic pathways of apoptosis and extrinsic pathway of apoptosis [34]......  | 19 |
| Figure 10: EGCG-capped nanoparticle synthesis and functionalization of T-Au-PEG-BA and T-Au-[PLL-g-PEG] BA nanoparticles [40]. .....   | 24 |
| Figure 11: Braggs Law. [42].....   | 29 |
| Figure 12: Working Principle of X-Ray Diffraction [43]. .....  | 29 |
| Figure 13: Schematic Diagram of Fourier-transform Infrared spectroscopy (FTIR) [44]......  | 30 |
| Figure 14: Raman Scattering [45]......   | 31 |
| Figure 15: Schematic Diagram of Raman Spectroscopy [46]......  | 32 |
| Figure 16: Schematic Diagram of UV-Vis Spectroscopy [47]. .....  | 33 |
| Figure 17: Apparatus used for gel electrophoresis.[48] .....   | 34 |
| Figure 18: (a) Schematic Diagram of Zeta Potential (b) folded capillary cell. [49] .....   | 35 |
| Figure 19: Synthesis of Gold Nanoparticles by Two Phase Method. ....   | 38 |
| Figure 20: PMA wrapped Hydrophobic Dodecanethiol Capped Gold Nanoparticles.....  | 40 |
| Figure 21: PEG Modified Polymer Coated Gold Nanoparticles.....   | 41 |
| Figure 22: Drug Loaded PEG Modified Polymer Coated Gold Nanoparticles. ....  | 42 |
| Figure 23: (a) Gold Nanoparticles;(b) Poly (methyl acrylate) (PMA) coated Gold Nanoparticle; (c) Betulinic Acid loaded Polymer coated Gold Nanoparticles. ....   | 44 |
| Figure 24: FTIR spectra (a) Betulinic Acid; (b) Polyethylene glycol (PEG) coated Gold Nanoparticles; (c) Betulinic Acid loaded Polymer coated Gold Nanoparticles. ....   | 45 |
| Figure 25: (a) Raman Spectrum of Betulinic Acid (BA); (b) Raman Spectrum of Betulinic Acid loaded Polymer coated Gold Nanoparticle. ....   | 46 |
| Figure 26: XRD of Gold Nanoparticles. ....   | 47 |
| Figure 27: XRD of PEG Modified Polymer Coated Gold Nanoparticles. ....   | 48 |
| Figure 28: Gel Electrophoresis of PEG Modified Polymer Coated Gold Nanoparticles and Betulinic Acid Loaded PEG Modified Polymer Coated Gold Nanoparticles. ....  | 49 |
| Figure 29: Zeta Potential: (a) PMA Coated Gold Nanoparticles at pH 5;(b) PEG Modified Poly (methyl acrylate) (PMA) coated Gold Nanoparticle at pH 5; (c) Betulinic Acid loaded Polymer coated Gold Nanoparticles at pH 5; (d) PMA Coated Gold Nanoparticles at pH 10;(e) PEG Modified Poly (methyl acrylate) (PMA) coated Gold Nanoparticle at pH 10; (f) Betulinic Acid loaded Polymer coated Gold Nanoparticles at pH 10. .... | 50 |

|  |           |
|--|-----------|
| <i>Figure 30: Antioxidant of PMA coated gold nanoparticles, PEG modified PMA coated gold nanoparticles, drug loaded gold nanoparticles and drug.....</i> | <i>51</i> |
| <i>Figure 31: Image of Antioxidant of PMA AuNPs and PMA PEG AuNPs .....</i>  | <i>52</i> |
| <i>Figure 32: Image of Antioxidant of Drug Loaded AuNPs and Drug.....</i>  | <i>52</i> |
| <i>Figure 33: Cytotoxicity Assessment on HEK 293T and MDA-MB-231 Cells by AUNPs-PMA. ....</i>  | <i>53</i> |
| <i>Figure 34: Cytotoxicity Assessment on HEK 293T and MDA-MB-231 Cells by AUNPs-PMA-PEG. ....</i>  | <i>54</i> |
| <i>Figure 35: Cytotoxicity Assessment on HEK 293T and MDA-MB-231 Cells by AUNPs-PMA-PEG. ....</i>  | <i>54</i> |

## **Tables**

|  |           |
|--|-----------|
| <i>Table 1 Different Drug Carrier[11] .....</i>      | <i>10</i> |
| <i>Table 2 Member of Bcl 2 Family.[34] .....</i>     | <i>20</i> |
| <i>Table 3 Antioxidant Activity of Samples .....</i> | <i>52</i> |

# Chapter 1

## Introduction

One of the leading causes of death in the world is cancer. The World Health Organization projects that 10 million individuals would lose their lives to cancer globally in 2020. Approximately 400,000 children develop cancer every year. An estimated 20 million new instances of cancer were reported worldwide. Over the next two decades, there will be an estimated 60% increase in the cancer burden.

Breast cancer is currently one of the most often diagnosed malignancies and the fifth leading cause of cancer-related deaths, GLOBOCAN 2020 predictions state that there will be 2.3 million additional cases globally.[1] In 2023, it is predicted that there will be 297,790 new cases of aggressive breast cancer in women and 2,800 new cases in men. Female breast cancer has surpassed lung cancer.

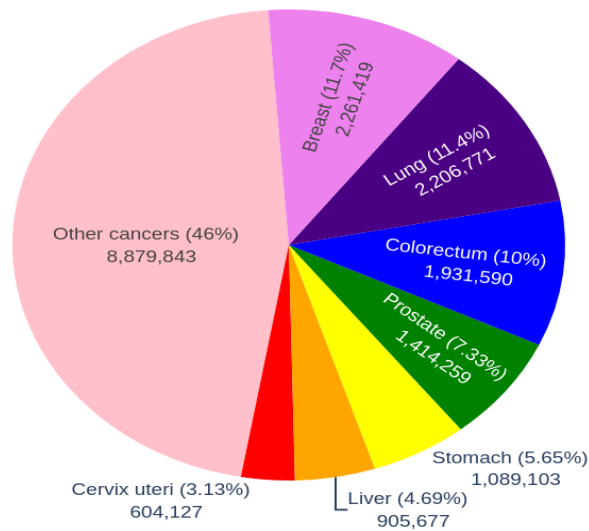


Figure 1: GLOBOCAN 2020 Statistic. [2]

### 1.1 What is Cancer?

Our bodies are made of trillions of tiny cells that form our tissues and organs. Normal cells grow, divide, age and die. Cancer cells resist every principle. They are rebels with a cause: they want to be immortal. Because cancer cells are immortal. An extreme example of this is what are known as "HeLa cells," which are genuine cancerous cells from Henrietta Lacks, a lady who died from

cervical cancer in 1951. Her malignant cells are still being employed in medical research for important purposes such as helping to develop the polio vaccine.

## ***1.2 Types of Cancer***

Cancer is divided into four main categories.

### *Carcinomas*

The term "carcinoma" refers to tumors that start in the skin or in the surface tissue of internal or glands and organs. Carcinomas frequently develop into solid cancer. They are the highest prevalent cancer type. Colorectal, breast, prostate and lung cancer are all examples of carcinomas.[3].

### *Sarcomas*

Sarcomas develop in the tissues that link and sustain the body. If not treated promptly, sarcoma can spread to all cells in the body. It can harm the muscles, bones, nervous system, and other organs [3].

### *Leukemia*

A blood cell malignancy known as leukemia is characterized by uncontrolled cell death and damage. Acute lymphocytic leukemia is one of the most common forms of leukemia.

Chronic myeloid leukemia Chronic lymphocytic leukemia and acute myeloid leukemia are the three types of leukemia [3].

### *Lymphomas*

Blood contains lymphocytes, which boost the body's immunity. They are present in the lymph nodes, bone marrow and spleen , and when malignant cells infect the lymphocytes, they spread to other parts of the body, as well as other tissues and organs. Lymphoma can travel to other parts of the body.

Non-Hodgkin lymphoma and Hodgkin lymphoma are the most common kinds of lymphoma [3].

### ***1.3 Main Causes of Cancers***

#### *Genetic Factor*

Genes are conveyed in the cell nucleus by the DNA molecules of the chromosomes. The sequence in which amino acids must be combined to form a certain protein is specified by a gene. After that, the protein executes the gene's function. The cell produces the specified protein in response to the activation of a gene. Gene mutations can cause cellular disruption by changing the amount or nature of proteins.

There are a couple of gene categories, which account for a tiny role in the total genetic repertoire. These genes significantly influenced the tumor initiation. In their typical state, they control the cell's life spans, or the precise series of events that causes a cell to grow and divide. Tumor suppressor genes stop this kind of growth from occurring, whereas proto-oncogenes encourage it.

When proto-oncogenes are altered, they can transform into cancerous oncogenes which promote abnormal growth. The proto-oncogene's encoded growth stimulatory protein may create excessive amounts or a highly active variant because of the mutations. When malignant suppressor genes are inactivated by mutations, they lead to cancer. The cell is thus deprived of vital brakes that stop aberrant development because of the loss of functional suppressor proteins.

For a malignant tumor to emerge, mutations in at least six of the originating cell's growth-controlling genes are required. A growing cell's ability to become aggressive or potential of migrate (metastasizing) throughout the body may be caused by other types of genes, which may contribute in the development of cancer.[4]

#### *Smoking*

Smoking increases the chance of bladder, cervix, larynx, esophageal, mouth, and other cancers in addition to lung cancer.[3]

#### *Chemicals*

Cancer is linked to exposure to industrial dyes, asbestos, and benzene.[3]

#### *Ionization Radiation*

Although a relationship has been established between ionizing radiation and cancer, the precise amount of radiation exposure that increases the risk of cancer remains unknown.[3]

### *Viruses*

Certain viruses, such as the HIV/AIDS virus and Acquired Immune Deficiency Syndrome, are responsible for raising the incidence of cancers such as liver carcinoma, lymphomas, and sarcomas. Cervical and anal cancers are caused by HPV viruses.[3]

### *Sunlight*

Long-term direct exposure to ultraviolet rays from the sun causes skin damage and may result in skin cancer.[3]

## **1.4 Breast Cancer**

The most typical carcinoma in women is cancer of the breast. The formation of breast cancer is a multi-step process involving multiple kinds of cells and prevention is still an international problem. Several risk factors, such as ageing, estrogen, gene mutations, an unhealthy lifestyle and family history might increase the chance of developing breast cancer. Breast cancer may travel to distant organs such as the liver, bone, lung, and brain since it is a metastatic illness, which explains how it is incurable. Early disease discovery can result in a good result and a high survival rate.[5]

The glandular cells and the stromal (supporting) cells make up two entirely different types of tissues which make up the breast. Stromal cells hold the breast's fat and fibrous connective tissues, and glandular cells hold the milk-producing glands (lobules) and ducts (the milk tubes). The breast contains the lymphatic tissue of the immune system, which eliminates waste products and cellular fluids.[6]

Various types of cancer can develop in various parts of the breast. Most breast malignancy is brought on by harmless changes. For example women suffering from fibrocystic change, a harmless situation, might experience lumpiness, areas of swelling, discomfort, or chest pain, tumors (collected packets of liquid), and fibrosis (growth of scar-like connective tissue). [6]

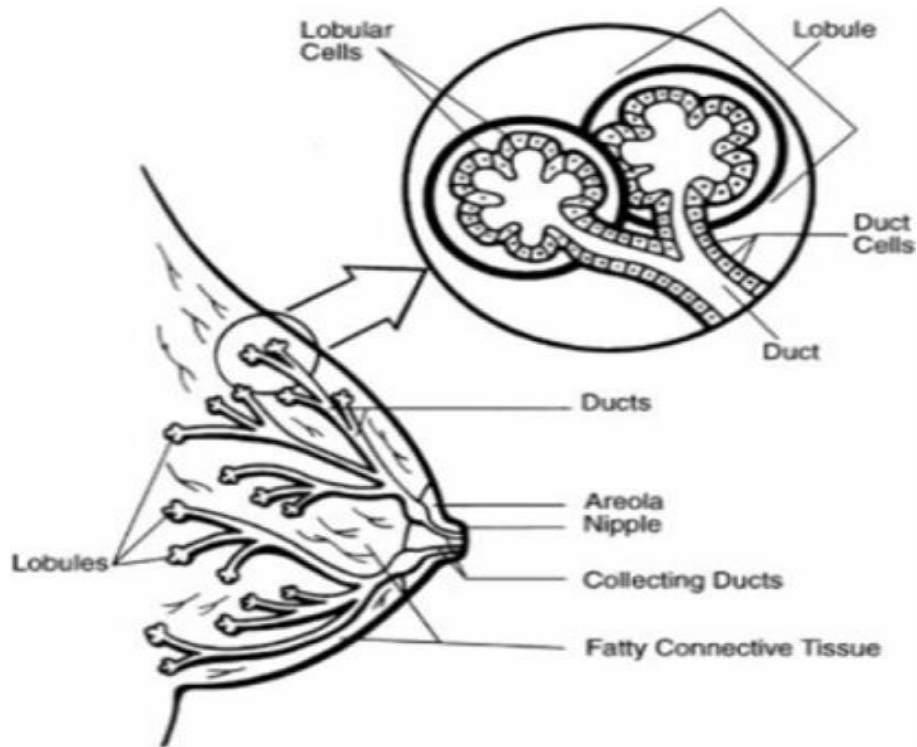


Figure 2: Anatomical diagram of the normal breast (mammary gland) showing the structure of glandular tissues, lobules and stromal tissue within the breast mound. [6]

The majority (lobular tumors) begin in the cells which form the lobules, whereas others develop in other tissues [6].

### ***1.5 Traditional Methods of Cancer Treatment***

Treatment options for patients with cancer are limited for many years, including radiation therapy, chemotherapy, and surgery either individually or in combination. These methods have many limitations. Chemotherapy is the most successful and extensively utilized cancer treatment technique, whether used alone or in combination with radiotherapy. Almost all chemotherapeutic medicines kill normal cells, especially those that proliferate and grow quickly, even though chemotherapy has decrease morbidity and mortality. Drug resistance, which happens when tumor cells that were initially suppressed by an anti-cancer treatment start to grow resistant to the medication, is another significant issue with chemotherapy. The main contributors to this are reduced medication absorption and enhanced drug efflux. The drawbacks of conventional chemotherapeutic methods are their challenging dosage selection, poor selectivity, quick drug metabolism, and mostly severe side effects. Surgery is most beneficial when the disease is in its

initial stages. Damage to healthy cells, tissues, and organs could result during radiation therapy. Drug delivery and resistance to drugs are the two biggest issues in the fight against cancer [7].

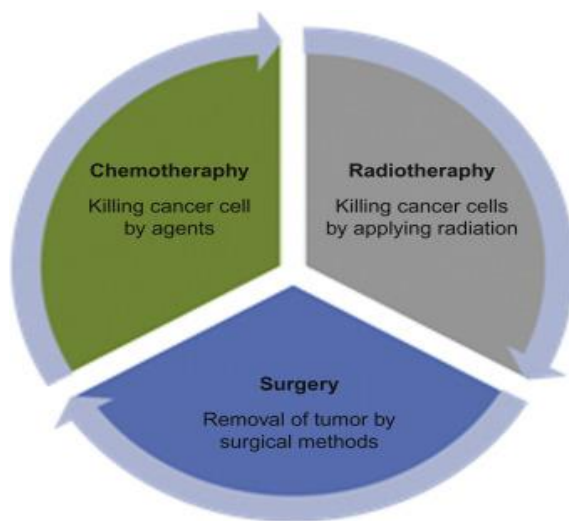


*Figure 3: Systematical diagram of traditional methods for cancer treatment [8]*

### ***1.6 Nanoparticles and Nanomedicine***

#### **Advance Methods in the Field of Cancer Treatment**

Nowadays much research is conducted to overcome many obstacles in cancer treatment like drug resistance and its delivery to active sites of cancer. Here are some examples of modern and innovative cancer therapies, along with a list of advantages and disadvantages.

#### ***Stem Cell Therapy***

In bone marrow, stem cells are cells with no differentiation that can develop into any type of body cell. Cancer therapy options using stem cell therapies are also known to be secure and efficient. Applications of stem cells remain in the experimental phase of clinical test; such application is the investigation of their potential for regenerating other wounded tissue. Clinical trials presently use mesenchymal stem cells (MSCs) obtained from adipose tissues, connective tissues, and bone marrow.

In general, cancer treatment employs stem cell therapy in a variety of ways, including HSC transplantation, MSC infusion, therapeutic carriers, immunological effector cell generation, and vaccine creation.

The following side effects were observed in the treatment of tumor by using stem cell therapy:



- (1) carcinogenesis
- (2) unfavorable outcomes after allogeneic HSC transplantation
- (3) drug toxicity
- (4) drug resistance
- (5) enhanced immunological responses and autoimmune
- (6) viral infection.[7]

### *Ablation Cancer Therapy*

Tumors can be removed without being removed using the therapy technique known as ablation. When surgery is not an option, it is mostly utilized for small tumors that are less than 3 cm in size. Ablation is paired with embolization for larger tumors. However, because it removes some of the surrounding healthy cells, this therapy might not be suitable for treating cancer close to major bile ducts, diaphragms, or blood vessels. [7]

### *Gene Therapy*

Gene therapy involves inserting a healthy duplicate of a damaged gene into the DNA to treat a particular illness. In individuals with severe immunodeficiency in multiple areas syndrome (SCID), the ADA gene was initially delivered to T cells using a retroviral vector in 1990. Currently, there are about 2900 clinical trials using gene therapy, with two-thirds of them focusing on cancer. Chemosensitizing and proapoptotic genes are produced, wild-type genes that suppress tumors are expressed, genes that may stimulate anti-cancer immunity are produced, and cancer genes are particularly silenced as therapies for cancer gene therapy.

The choosing of the ideal conditions and the most effective delivery method have been some of the issues with gene therapy. Genome integration, limited effectiveness in specific patient subsets, and a sizable danger of immunity neutralization have all been listed as this therapy's drawbacks. [7]

### *Natural Antioxidants*

The anatomy experiences several external insults every day, including ultraviolet rays, tobacco smoke and pollution which lead to the buildup of reactive species, especially free radicals, and

oxidants, which are too responsible for the start of numerous illnesses, especially cancer. However, these molecules are also formed naturally inside our tissues and cells by mitochondria and peroxisomes, and by macrophage metabolism, as a component of the natural physiological aerobic process. These substances are also produced through the administration of therapeutic medications.

In addition to their antioxidant and anti-inflammatory properties, natural antioxidants like polyphenols, vitamins and bioactive compounds produced from plants are employed as preventive and medical remedies against these harmful substances. Research has been incorporated to cancer therapy because of their proapoptotic and anti-proliferative properties. Natural antioxidants that have undergone in vitro as well as in vivo testing include vitamins, flavonoids, alkaloids, quercetin, turmeric, carotenoids and more.

Toxicity and low bioavailability of natural drugs is one challenge in implementing them into medical practice. While protecting normal cells at therapeutically effective doses, curcumin exerts deadly effects on a variety of cancer types, including lung, brain, leukemia, tumors of the pancreas, and cancer of the liver. Investigations are being done into the biological properties of curcumin, how long it takes to treat patients, and the best therapeutic doses. Approximately 27 clinical trials are now underway, with another 40 under investigation for curcumin.[7]

### *Targeted Drug Delivery*

Among all these methods, the targeted drug delivery method can solve many problems. Targeted drug delivery, the undesirable side effects of conventional drug administration can be avoided, and the dosage needed for therapeutic efficacy can be lowered while still delivering the drug component specifically to the organ, cells, and intracellular level of the intended body region. Drug Delivery Systems (DDSs) are classified into five generations, with targeted delivery being the fourth.

The concept of targeting the drug to the active sites is taken from the magic bullet concept. More than a century ago, Paul Ehrlich suggested using "magic bullets" to target a virus in a specific way without damaging the host organism. For more than a century, scientists were compelled to study more, due to this fascinating idea which help the discovery of several nm-scale devices, today known as "nanomedicines." This concept is very good but there are many problems for implementing the magic bullet to clinical trial. This is a result of the difficulties in determining the

best targeted therapy for a particular illness state, the medication that effectively cures the sickness, and the ways to deliver the medicine in a stable form to specific locations while avoiding immune-stimulating and unexpected interactions [9].

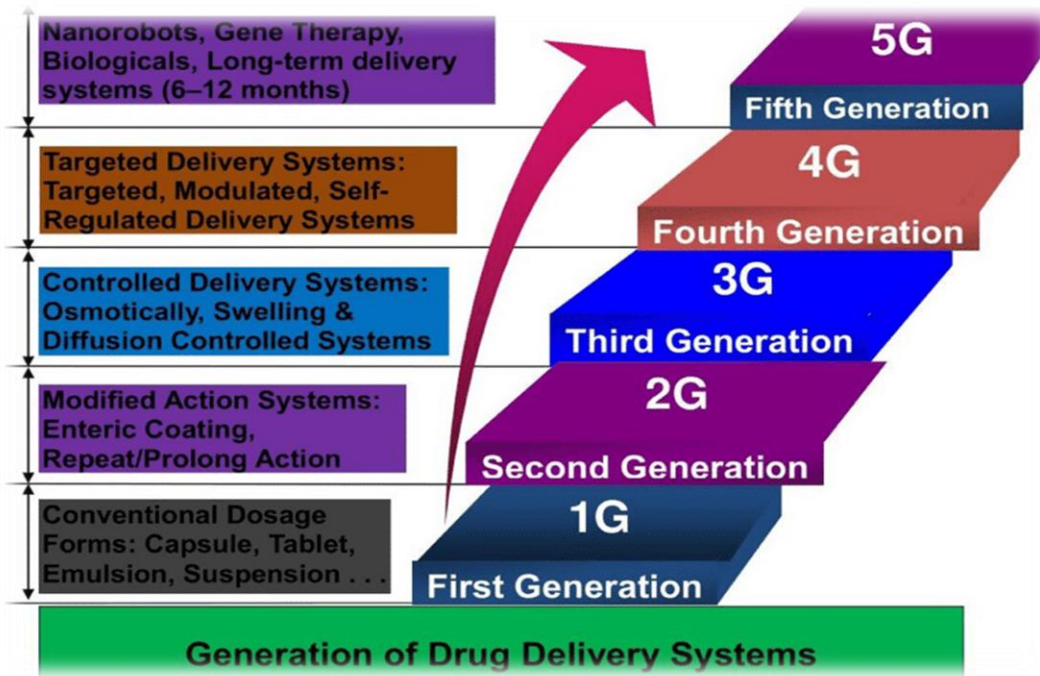


Figure 4: Generation of Drug Delivery System. [9]

#### Carriers used for Targeted Drug Delivery

In recent years, numerous inorganic materials like nonmetallic and metal nanoparticles and organic materials for example natural polymers, exosomes, liposomes, and dendrimers have been investigated as delivery carriers and developed into multifunctional drug delivery systems with the best shape, surface properties and size to maximize the antitumor effect.

Metals are naturally occurring elements on Earth and are widely used in industries, agriculture, medicine, and daily life. Metals have been used to create metal nanoparticles as well. The most popular materials utilized to make metallic nanoparticles include gold, silver, zinc, iron, and aluminum. They are synthesis by mechanical attrition, coprecipitation, laser ablation, sol gel method, photo reduction, chemical electrolysis, and synthesis organisms like bacteria, fungi, and plants. Metallic nanoparticles are extensively utilized in fields like food, agriculture, engineering, biology, medicine, and cosmetics. In addition to having their own distinctive physicochemical characteristics, they also have antimicrobial, anticancer, catalyzing, optical, electronic, and

magnetic properties. They are also utilized in food and biomedical devices. The unique properties of metallic nanoparticles make them the perfect candidate for targeted delivery of drug. Surface of metallic nanoparticles can also be functionalized with different polymers. We can also control the shape and size [10].

*Table 1 Different Drug Carrier[11]*

| <b>Sr No</b> | <b>Nanocarriers</b>              | <b>Advantages</b>   | <b>Disadvantages</b>  |
|--------------|----------------------------------|---|---|
| 1            | Liposomes[12]                    | <ul style="list-style-type: none"> <li>• Biocompatible and biodegradable</li> <li>• Capable of encasing bioactive substances</li> <li>• Drug entrapment</li> <li>• Extended release</li> </ul>              | <ul style="list-style-type: none"> <li>• Low stability</li> <li>• Tends to aggregate.</li> <li>• Allergic</li> </ul>                      |
| 2            | Gold nanoparticles[13]           | <ul style="list-style-type: none"> <li>• Biocompatible</li> <li>• Ease of synthesis</li> <li>• Combining more than one agent</li> <li>• Particle size</li> </ul>  | <ul style="list-style-type: none"> <li>• Not biodegradable</li> <li>• Expensive production</li> <li>• Nanoparticle agglomerate</li> </ul> |
| 3            | Quantum dots[14]                 | <ul style="list-style-type: none"> <li>• Imaging applications</li> <li>• Theranostic properties</li> <li>• Particle size</li> </ul>   | <ul style="list-style-type: none"> <li>• toxicity</li> <li>• Instability</li> <li>• Agglomeration</li> </ul>                              |
| 4            | Polymeric nanoparticles [15, 16] | <ul style="list-style-type: none"> <li>• Controlled</li> <li>• Stability</li> <li>• Control drug release</li> <li>• Flexibility</li> <li>• Accumulates in tumors</li> </ul>                                 | <ul style="list-style-type: none"> <li>• Aggregation</li> <li>• Nanotoxicity</li> </ul>   |
| 5            | Dendrimers[17, 18]               | <ul style="list-style-type: none"> <li>• Water soluble</li> <li>• Biocompatible</li> <li>• PK behavior</li> <li>• Flexibility in conjugation</li> <li>• Ability to encapsulate bioactive agents.</li> </ul> | <ul style="list-style-type: none"> <li>• Poor drug release</li> <li>• Toxicity</li> <li>• Rapid clearance</li> </ul>                      |
| 6            | Carbon nanotubes[19]             | <ul style="list-style-type: none"> <li>• Ease of synthesis</li> <li>• Conjugation of bioactive agents</li> <li>• Large surface area</li> <li>• Protects entrapped drug.</li> </ul>                          | <ul style="list-style-type: none"> <li>• Poorly solubility</li> <li>• Non-biodegradable</li> <li>• Toxicity</li> </ul>                    |

### ***1.7 Gold Nanoparticles***

Several unusual optical, electrical, sensing, and biological capabilities, Au NPs have long been regarded as the most fascinating nanoparticles. The potential applications of Au NPs in disease detection, diagnosis, and treatment include cancer therapy, drug administration, and medical imaging.

We can readily synthesize sphere like, rod-like, cage-like Au NPs having diameters that vary from 1 nm to more than 100 nm. Au NPs' optical and electrical characteristics are heavily influenced by their shape and size. One of the most frequent gold nanostructures used in medication administration is spherical gold nanoparticles. Another gold nanostructure that is widely used in photothermal application is gold nano rods. They are also extensively used in near infrared (NIR) applications[20].

Surface functionalization is one of the main advantageous characteristics of Au NPs in the biological area. Surface of Au NPs can be functionalized with, numerous biomolecules, including peptides, antibodies, Deoxyribonucleic acid (DNA). Interaction is classified into two types, noncovalent interactions, covalent interactions [20].

Van der Waals forces, hydrophobic trapping, and electrostatic interactions are all involved in noncovalent modifications. The benefit of this relationship is that the biomolecule cannot be connected to diverse chemical changes that could jeopardize its main, active state. However, binding itself is insufficient to generate long-lasting surfaces that can endure the necessary washing procedures and incubation conditions, especially in biological research. When employing this modification, it is critical to consider the pH and ionic strength of the media in question [20].

Covalent modifications are extremely stable under heat settings and can resist very high salt concentrations. Covalent alterations, on the other hand, are typically more complex, necessitating extensive ligand synthesis [20].

Au NPs have demonstrated a high potential for usage as drug delivery vehicles. Gold nanoparticles can transport a variety of therapeutic compounds, synthetic proteins, vaccines, or DNA into their intended sites and control release of drugs by internal biological signals or external light stimulation.

Conjugates of gold nanoparticles with medicinal molecules are very useful in the treatment of end cellular disorders. They have the potential to boost therapeutic efficacy. Antibiotics and other therapeutic compounds can directly combine with gold nanoparticles by covalent interaction and ionic interactions , as well as physical absorption [20].

Enhancing the efficacy of treatment is significantly impacted by the spatiotemporal release of a payload. Because of their distinct chemical and electrical, physical, and optical characteristics, gold nanoparticles can be employed in novel ways to control drugs distribution and release. When the gold nanoparticles are exposed to either internal or external stimuli, such as light, glutathione, or pH, the medicine is released. [20]

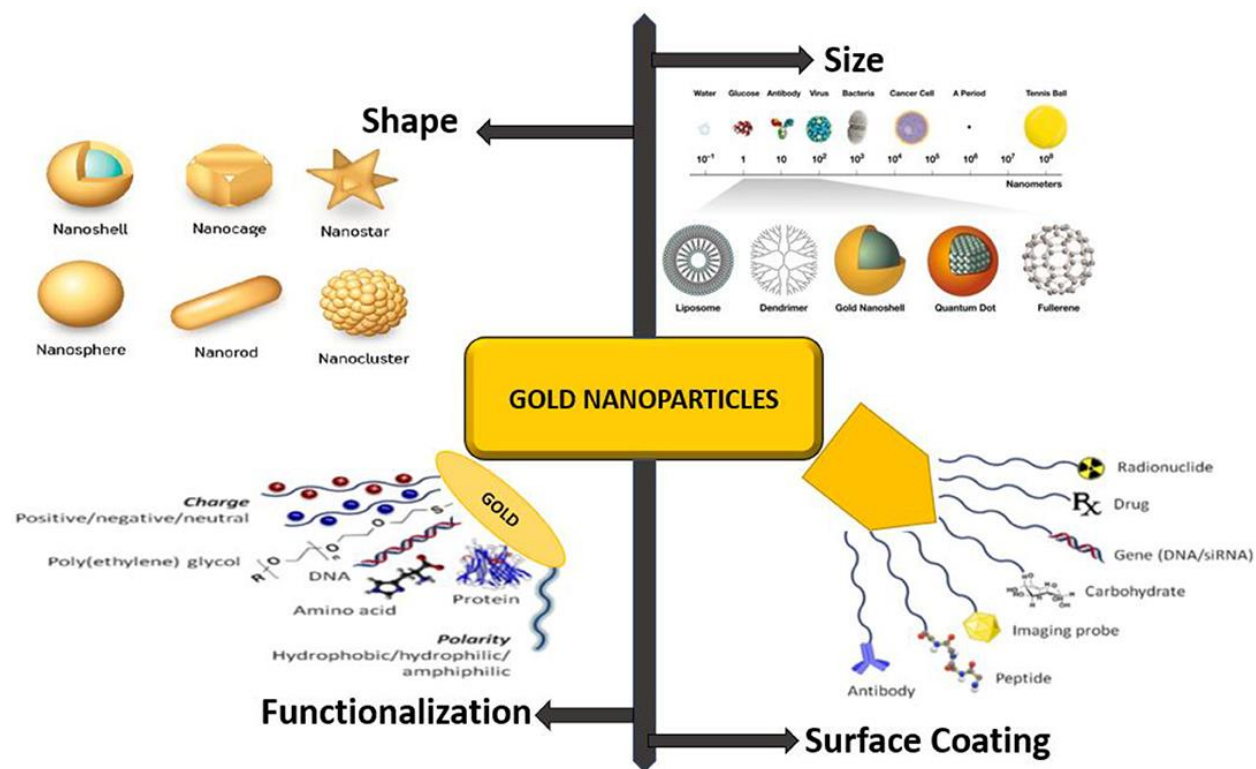


Figure 5: Different Advantages of Using Gold Nanoparticles .[21]

Au nanoparticles are safe and biocompatible. Surface plasmon resonance bands, extremely small size, the macroscopic quantum tunnelling effect, and the surface effect of Au NPs all make them stand out. These distinct characteristics have made Au NPs the most attractive material for a variety of biological applications, such as biosensors, molecular imaging, drug carriers, and so forth. [20]

### *Surface Plasmonic Resonance (SPR)*

Surface Plasmonic Resonance is a quantum electromagnetic phenomenon that takes place at the metal-dielectric contact when light interacts with free electrons. An optical process takes place when a monochromatic, p-polarized light beam collides with a metal surface (often gold).

When resonance conditions are met and the frequency of the incident light coincides with the surface plasmon wave frequency at a specific incidence angle, Some of the light energy is converted to electron energy packets on the surface of the metal. The detected reflected light then becomes less intense. Electron coherent oscillations called surface plasmons (SPs) are induced by the exponentially decreasing evanescent field of incident light and move parallel to the metallic surface. The resonance angle, sometimes referred to as the SPR-dip, is the angle at which the highest intensity of the reflected light is lost.[22]

When the size of a metallic nanoparticle is smaller than or equal to the electron mean free path, which is roughly equal to 100 nm, new properties become apparent in comparison to bulk materials because of restrictions on electron motion. For example, when an oscillating electric field from the propagation of light passes through a metal nanoparticle, the free conduction band electron oscillates. This collective resonance oscillation of electrons confirmed in nanoparticles this is called localized surface plasmon resonance. The reason why colloidal nanoparticles exhibit vibrant colors is because the nanoparticle can give high scattering and absorption if the electron's frequency matches that of light. The colour depends on the surface plasmonic wavelength.

Plasmons are metal-based collective oscillations of free electrons. A 'plasmon' is referred to as a bosonic quasiparticle excitation and equates to a quantum of plasma oscillation because these oscillations happen at a constant frequency. Plasmons are defined as a negatively charged electron cloud that is coherently displaced from its equilibrium location around a lattice of positively charged ions, in accordance with the Fermi liquid model. This is similar to how real plasma is described. [23]

Charges are separated with regard to the ionic lattice as a result of this electron mobility over the particle surface leading to a dipole to fluctuate in the electric field of the light. Surface plasmon

resonance is a phenomenon where the oscillation's amplitude is greatest at a particular frequency.

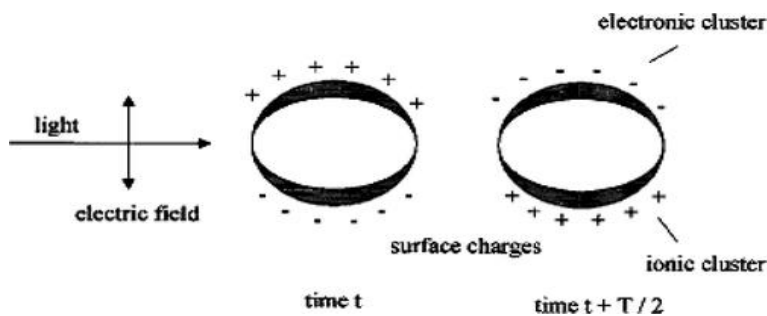


Figure 6: The interaction of electromagnetic radiation with the metal sphere causes the formation of surface plasmons in metallic nanoparticles. A dipole is created, which oscillates in phase with the incoming light's electric field.[24]

A UV-Vis absorption spectrometer can measure the SPR since it generates high incident light absorption. Noble metals, especially gold and silver, which are plasmonic nanoparticles have an SPR band that is noticeably stronger than that of other metals. According to Mie theory, the electron charge density on the particle surface is influenced by several factors, including the type of metal, the size, shape, and composition of the particles as well as the surrounding medium's dielectric constant. These factors ultimately determine the wavelength and intensity of the SPR band. [25]

In the visible area, gold NPs exhibit the SPR band of about 520 nm. Particle size influences the Surface Plasmonic Resonance band. The SPR band of gold NPs smaller than 10 nm is considerably decreased due to phase changes caused by greater electron-surface collision rates relative to bigger particles. The Surface Plasmonic Resonance wavelength is redshifted and intensified as particle size increases. Band broadening is noticeable for particles larger than 100 nm due to the dominance of higher order electron oscillation. [26, 27]

#### *Surface plasmon absorption and scattering*

Two processes, absorption, and scattering are responsible for an EM wave's energy loss (complete light extinction) after passing through a medium. When the energy of photons is lost due to inelastic processes, light is absorbed. When the energy of photons causes electron fluctuations in materials, this process is known as light scattering. Rayleigh scattering and Raman scattering are the two types of light scattering that can occur. The shift in frequency relates to the energy



differential brought on by the rotation, stretching, or vibration of molecules within matter. The Surface Plasmonic Resonance oscillation dramatically increases. It is 5-7 orders of magnitude larger than the bulk of strongly absorbing organic dye molecules and the emission of most vividly fluorescent compounds in terms of both light absorption and scattering. [27, 28]

The efficiency of total extinction, scattering, and absorption of surface plasmons is often investigated using full Mie theory. [25] Higher order electron fluctuations are the reason for this. These fluctuations start to play critical roles for nanoparticles larger than 20 nm, and light absorption as well as scattering is clarified by considering all multiple fluctuations. About 100 percent of the total attenuation for a 20 nm gold NP can be explained by absorption. When the dimension is increased to 40 nano meters, scattering begins to appear. Extinction results from equal amounts of scattering and absorption at a size of 80 nm. The quantitative connection shows that the ratio of scattering to absorption rises noticeably with increasing particle size. This fact should be considered while selecting Au Np for biomedical purposes. As light is absorbed largely by smaller nanoparticles, they are chosen for use in photothermal therapy, effectively converting it to heat for tissue and cell death, whereas larger nanoparticles are preferred for imaging due to improved scattering effectiveness. [27, 28]

### ***1.8 Apoptosis***

"Apoptosis" is derived from the ancient Greek word, which means the "falling off petals from a flower" or the "dropping off leaves from a tree in autumn." John Kerr introduced the name for the first time in 1972. Apoptosis is the predetermined process of cell death. Unwanted cells are removed early in the development process using it. Additionally, apoptosis helps in the suppression of cancer. [29]

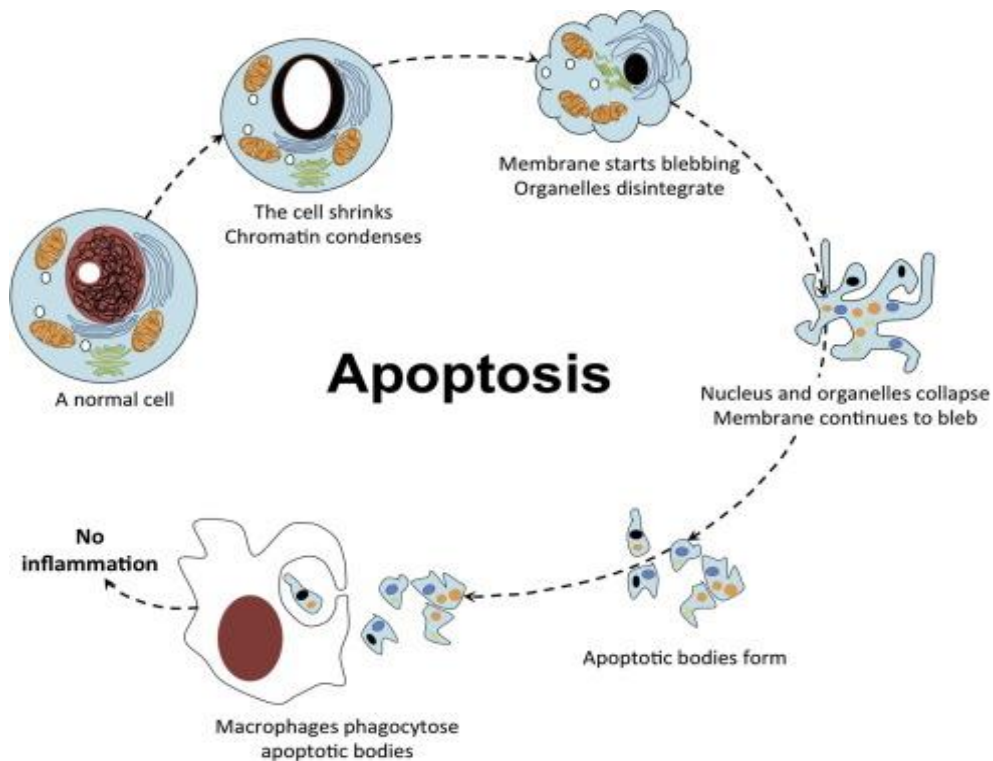


*Figure 7: Different steps of apoptosis. Start with cellular shrinkage than membrane oligomerization and nucleus collapse at the end apoptotic bodies form which are eventually engulfed by macrophages. [30]*

As shown in the above figure Apoptosis, is the process of cell death without inflaming itself by packing up all its contents and delivering them to be consumed by nearby cells. Apoptosis can start because of signals emanating from inside the cell (intrinsic/mitochondrial apoptosis) or from outside the cell (extrinsic apoptosis). [30]

### *Role of Mitochondria in Apoptosis*

Cell organelles called mitochondria, which are membrane-bound, generate most of the chemical energy needed to power a cell's metabolic processes. It is also known as the powerhouse of cells. The microscopic molecule known as adenosine triphosphate (ATP) stores the chemical energy produced by the mitochondria. It has a significant impact on the apoptotic process.

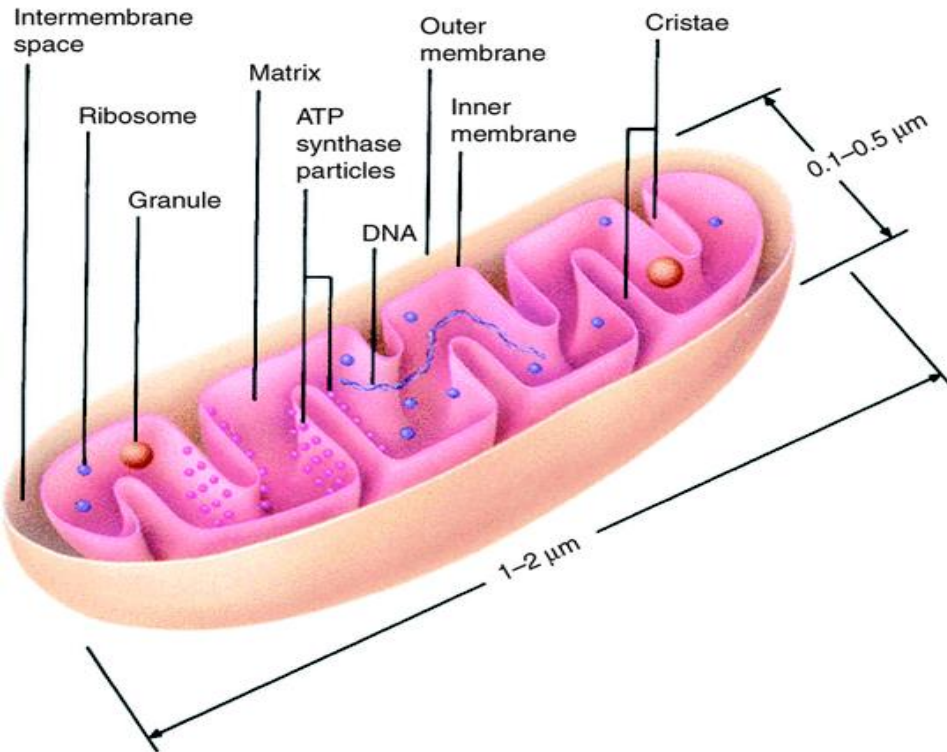


Figure 8: Structure of Mitochondria [31].

Mitochondria are essential for the activation of caspase because they release cytochrome C. [32]

### *Pathways of Apoptosis*

There are two types of pathways.

- 1 Extrinsic pathway
- 2 Intrinsic pathway

### *Extrinsic pathway*

The death receptor (DR) Fas receptor (CD95, tumor necrosis factor receptor) is found on the surface of many different cells and initiates a signal transduction cascade that results in apoptosis. Several biological and the association of Fas with its receptor ligand FasL (FasL/CD95L) regulates pathogenic events that result from programmed cell death. [33] Death receptors can cause apoptosis indirectly by increasing the death signal via activating the intrinsic/mitochondrial pathway or directly by activating caspases, which will cause apoptosis. There is a common extracellular death receptor domain (DR) on every Fas receptor, and when FasL attaches to it, it

causes the death receptors to oligomerize and set off a series of processes that cause the target cells to go into apoptosis. The procaspase and FADD both contain the death effector domain (DED), is employed by FADD to bind, through the death domain (DD), the Fas-associated death domain (FADD) adaptor molecule. FADD then forming the death-inducing signaling complex (DISC), a complex comprising the initiator procaspase-8 and procaspase-10, which is composed of both FADD and the procaspase. DISC complex activates Procaspase-10 and Procaspase-8. where they are autoproteolytically cleaved and activated, resulting in the activation of the effector caspases. [34]

In fully developed lymphocytes, Fas expression is strong, that have been activated as well as in lymphocytes that either have the human T-cell leukemia virus (HTLV-I) or the human immunodeficiency virus (HIV) infection. Fas is essential for T-cell mediated toxicity. It is thought that the removal of virus-infected cells or undesired activated lymphocytes depends on the Fas apoptotic pathway.

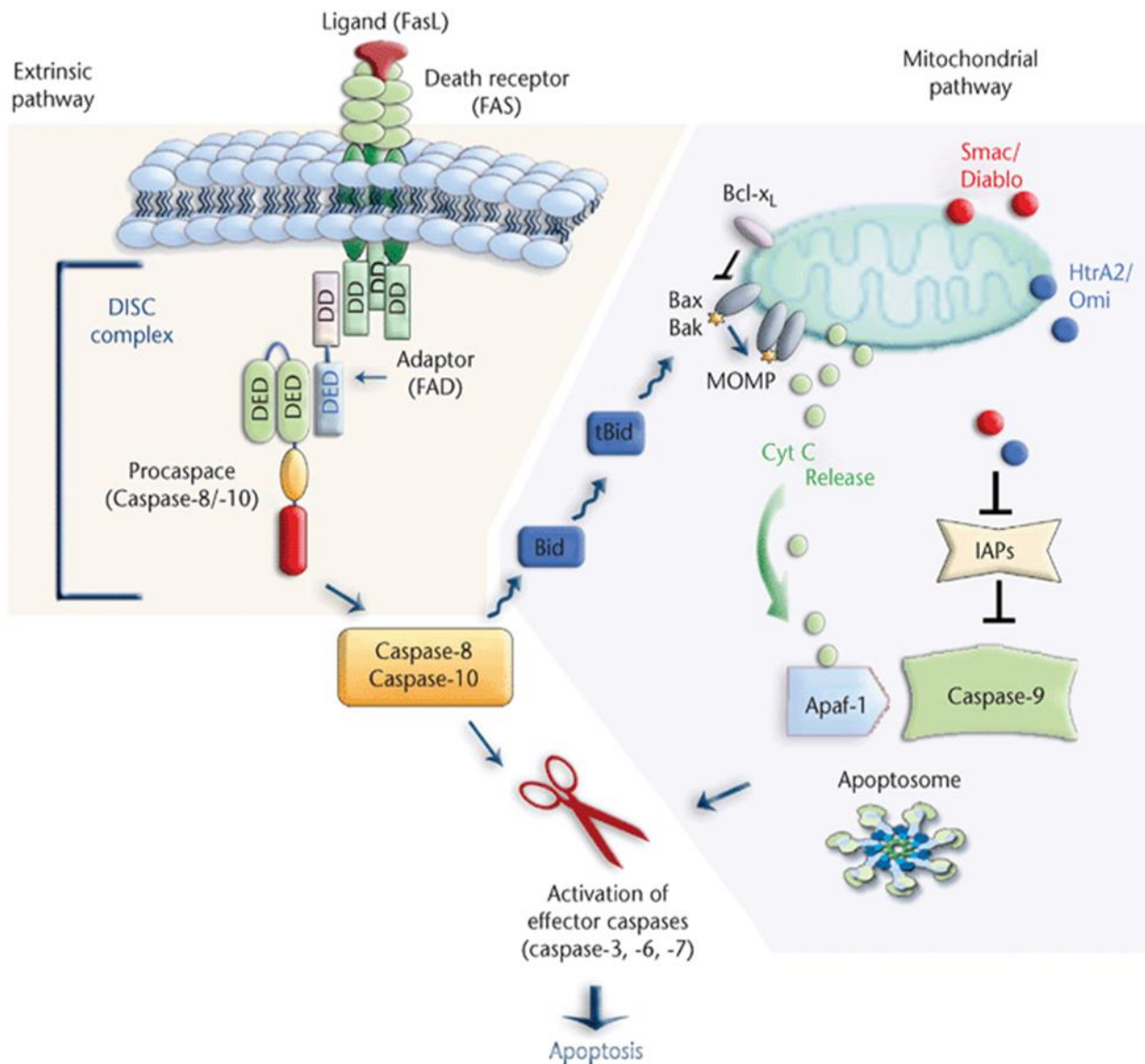


Figure 9: Intrinsic pathways of apoptosis and extrinsic pathway of apoptosis [34].

### Intrinsic or Mitochondrial Pathway of Apoptosis

A crucial part of the intrinsic path is the Bcl-2 family of proteins. The Bcl-2 family members act as important apoptotic regulators by linking the intrinsic and extrinsic pathways. There are currently 23 known members of the Bcl-2 family in humans. The Bcl-2 family members can be categorized into three groups based on their functions and the type and quantity of BH protein domains they possess: proapoptotic proteins with BH3-only domains, proteins that inhibit apoptosis and have multiple BH domains (BH1-BH4), and proapoptotic proteins with multiple domains (BH1-BH4). [34]

*Table 2 Member of Bcl 2 Family.[34]*

| <b>FUNCTION IN APOPTOSIS</b> | <b>DOMAIN</b> | <b>FAMILY MEMBERS</b> |
|------------------------------|---------------|-----------------------|
| <b>Proapoptotic</b>          | BH3-only      | Bid, Bad, Bim, Puma   |
| <b>Proapoptotic</b>          | Multiple      | Bak, Bok, Bax         |
| <b>Antiapoptotic</b>         | Multiple      | Bcl-2, Bcl-xL, Mcl-1  |

In non-apoptotic cells, the proapoptotic multidomain members (Bax) bind to and are neutralized by members of the antiapoptotic multidomain, like Bcl-2. The BH3-only domain proteins react to signals causing cell death by deactivating the antiapoptotic multidomain proteins., breaking the inhibitory link between the proapoptotic and antiapoptotic proteins. The outer membrane of the mitochondria becomes damaged when proapoptotic Bcl-2 family members oligomerize that let cytochrome c out into the cytoplasm, which activates caspases and causes cell death. [34]

#### *Cytochrome C Release and Formation of Apoptosome*

Cytochrome c, a component of the electron transfer chain in mitochondria, is released in response to apoptotic stimuli and moves to the cytosol where it interacts with the companion protein Apaf-1, causing it to oligomerize and attract caspase-9 to create the apoptosome. As a result, the related caspase-9 is activated, which cleaves and activates the executioner caspase-3 and -7. Then, these cleave crucial cell substrates to create the cellular and metabolic processes known as apoptosis.

Inhibitor of apoptosis proteins (IAPs), which are natural inhibitors of caspases, become inactive by other released proteins (Smac/Diablo/Omi and Htr2), which enhance caspase activation. Although activated executioner caspases unmistakably cause cell death through apoptosis, inhibition of these proteinases only provides temporary protection; once the mitochondria permeabilize, death will occur regardless of caspase activation, either as a result of other toxic mediators released from the mitochondria or eventually due to the loss of vital mitochondrial functions. [35]

#### ***1.9 Betulinic acid***

A pentacyclic triterpenoid with plant origins, betulinic acid (3, hydroxy-lup-20(29)-en-28-oic acid) is extensively dispersed in the plant kingdom all over the world. There are several biological effects of betulinic acid. For example, it is widely used for its antitumor activity. The cytotoxicity of

betulinic acid is its capacity to cause cancer cells to undergo the mitochondrial pathway of apoptosis. Additionally, it has been utilized for its antibacterial, antiviral, anti-inflammatory, anthelmintic, anti-HIV, anti-malarial, anti-bacterial, and antioxidant qualities [36].

## ***Chapter 2***

### ***Literature review***

(D. A. Nedopekina et al., 2017) reported to increase several new combinations of betulinic and ursolic acids with a lipophilic triphenylphosphonium cation have been developed to address the mitochondriotropic effects and bioavailability of naturally occurring triterpenes. Three cancerous human cell lines (HCT-116, TET21N and MCF-7) were used in in vitro experiments, and it was found that all the triterpene acid derivatives were significantly more effective at inducing mitochondria-dependent apoptosis than betulinic acid. Several apoptosis indicators, such as the release of cytochrome c and the triggering of caspase-3 activity, were used to confirm this. The IC<sub>50</sub> was significantly less than BA.

The efficacy and selection of mitochondria-targeted cancer prevention medicines have recently been improved by association with a lipophilic mitochondriotropic triphenylphosphonium cation (TPP<sup>+</sup>). Enhancing mitochondrial targeting by combining a chemical with TPP<sup>+</sup> that has three positive charges enables the medicine to be used in lower doses. Because mitochondria have a relatively high transmembrane potential in compared to other cells and organelles, this organelle type is known to accumulate lipophilic cationic substances in a selective manner. Additionally, solid tumor cells have mitochondria with a larger transmembrane potential than normal cells, which may help explain why antitumor agents can be cytotoxic against tumor cells.

Conjugation of triterpenoids, ursolic acids and betulinic acid with a TPP<sup>+</sup> group, the cytotoxicity of malignancies was dramatically boosted when compared with BA. As determined by a variety of apoptosis markers, including cytochrome c release, induction of caspase-3 activity, and cleavage of poly (ADP-ribose) polymerase, the mitochondriotropic analogues of BA were significantly more effective at inducing mitochondria-dependent death than the original triterpenoid. Therefore, attachment with TPP<sup>+</sup> results in structural changes to BA that greatly enhance its anticancer properties. [37]

(S. Lu et al., 2020) reported Multiple-functioned engineered nanoparticles have drawn a lot of interest as drug delivery vehicles because they can get around numerous barriers to focused medication delivery. Out of 2500 plant extracts, BA was found to be the most effective antitumor agent. In vitro studies have shown that BA can cause the death of many different types of tumor



cells, including those from the pancreas, the breast, the hepatoma, the glioma, the leukemia, the ovary, the cervix, the prostate, the lung, and the colorectal malignancies. Despite BA's high biological activity, its limited water solubility and brief half-life in the systemic circulation limit its anticancer and therapeutic efficacies.

Thus, Nano Drug Delivery Systems are suggested as a solution to these problems. Until now, numerous NDDSs of BA have been described for their improved efficacy, including cyclodextrin inclusion complexes, liposomes, and nanoparticles. The simplest way to make hydrophobic BA more soluble and have a measurable impact on boosting the efficacy is to use cyclodextrin formulation. Cyclodextrins work efficiently to dissolve hydrophobic drugs. Its outer edge is hydrophilic while its inner hollow is hydrophobic. The solubility of BA can be increased by effectively enclosing molecules that are hydrophobic in its hydrophobic inner chamber. To guarantee that the produced NPs have beneficial functioning, gelatin is also added to the NDDSs. Animal skin and connective tissues naturally contain gelatin, a typical sustainable based on proteins biomaterial with the unique advantages of being highly soluble and low in antigenicity.

Oxidized dextran is used as the cross-linking agent to cause gelatin to link together on the surface of TiO<sub>2</sub> particles, creating a hydrogel layer. The inner cores are made from precursor particles of TiO<sub>2</sub>. The gelatin chains are coupled with inclusion complexes of betulinic acid (BA) and ethylenediamine-cyclodextrin. The addition of -cyclodextrin to the produced nanoparticles will boost BA's solubility and bioavailability. Due to their dual-targeted functionalized groups, betulinic acid/gelatin-cyclodextrin nanoparticles (BA/GGNPs) exhibit a stronger anticancer impact in vivo than (BA/GCD).

The BA/GGNPs created in this study might be effectively taken up by 4T1 cells and had an average particle size of 200–300 nm. Additionally, in both in vitro and in vivo anticancer tests, BA/GGNPs significantly inhibited 4T1 cells. Because GCD and gelatin were added, the anticancer effect of BA/GGNPs was significantly greater than the effects of pure BA and BA/GCD. In conclusion, the generated GGNPs' NDDSs are an effective way to load drugs into BA further increasing the bioavailability and anticancer activity of BA while having low toxicity and great biocompatibility. [38]

**(F. Amin, D. A. Yushchenko, J. M. Montenegro, and W. J. J. C. Parak et al.,2012)** reported inorganic colloidal nanoparticles (NPs) with hydrophobic caps, such as quantum dots,

superparamagnetic iron oxides and other magnetic NPs, or gold NPs, can now be easily added to aqueous solutions using the polymer-coating technique. The exact chemical make-up of the initial capping molecules is not necessary for the coating of hydrophobic NPs with an amphiphilic polymer since hydrophobic contact drives the process. The remarkable colloidal stability of polymer-coated NPs has been demonstrated. The polymer shell has recently been subject to extensive analysis and optimization. Organic fluorophores can be attached to the polymer shell surrounding the Nanoparticles by bioconjugate methods, or they can be integrated directly into the polymer and hence not immediately on the NP surface. As a result, NPs that lack fluorescence by nature, such FePt NPs, can be converted to exhibit fluorescence. [39]

(O. Oladimeji, J. Akinyelu, A. Daniels, and M. J. I. j. o. m. s. Singh et al., 2021) reported that as nanomedicine has developed, nanoparticles (NPs) have been modified for internal delivery for increased beneficial impact while reducing negative effects. They compared the effects of polyethylene glycol (PEG) and poly-L-lysine-graft-polyethylene glycol (PLL-g-PEG) copolymer on the effectiveness of the targeted delivery of betulinic acid (BA) to the mitochondria via epigallocatechin gallate capped gold nanoparticles with mitochondriotropic TPP+ modification. EGCG, was used to reduce Au (III) chloride to create EGCG-capped NPs, as shown in Figure. When EGCG-capped NPs were surface functionalized, Two polymer-coated variants were produced by applying both Polyethylene Glycol or a grafted polymer of PLL-G-PEG., the Au-[PLL-g-PEG] NPs, and Au PEG. The medication BA was conjugated with the (TPP+) for improved mitochondrial localization.

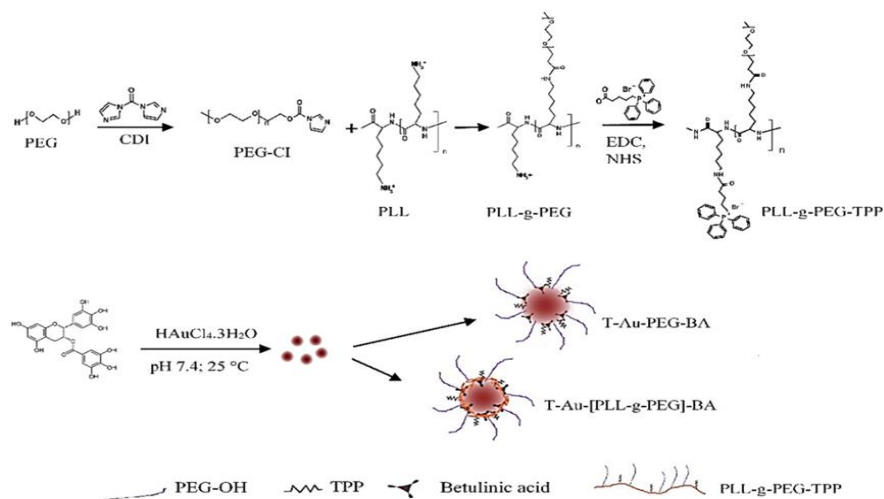


Figure 10: EGCG-capped nanoparticle synthesis and functionalization of T-Au-PEG-BA and T-Au-[PLL-g-PEG] BA nanoparticles [40].

Both T-Au-[PLL-g-PEG]-BA and T-Au-PEG-BA exhibited significant effects with little perceptible side effects in normal cells at lower dosages. When compared to the free drug, they markedly boosted toxicity in cancer cell lines. The most successful of the nanocomplexes was T-Au-[PLL-g-PEG]-BA, whose underlying mechanism involves the apoptotic pathway that is dependent on mitochondria. EGCG-capped NPs' potential usefulness as a platform for mitochondrial-targeted drug delivery was shown by the laminin receptor-dependent absorption of these particles [40].

**(C. A. J. Lin et al)** reported that several groups have also employed amphiphilic polymers to distribute hydrophobic nanoparticles in aqueous solutions. Biological molecules can be attached covalently to the surface of polymer, this class of hydrophilic particle coatings not only provides a flexible platform for the nanoparticles' chemical modification and bioconjugation, but also facilitates their phase transfer from organic solvents to aqueous solution.

To form a bond with the surface of the hydrophobic inorganic nanoparticles, amphiphilic polymers that are used to coat them usually have hydrophobic side chains. In addition, they have a hydrophilic backbone that acts as a stable foundation for the binding of biological molecules via bioconjugate chemistry and guarantees water solubility through charged groups, often  $\text{COO}^-$ .

Amphiphilic polymer covering for nanoparticles is a simple one-pot synthesis of a comb-like polymer that may be tailored to contain functional molecules directly without the need for crosslinkers, or to change its hydrophobic side chains. This strategy provides a flexible and dependable way to effectively introduce hydrophobic nanoparticles into aqueous solutions and to alter them using functional chemicals. [41]

## ***Chapter 3***

### ***Apparatus and characterization techniques***

The equipment and characterization methods utilized in the manufacture of drug-loaded gold nanoparticles will be briefly covered in this chapter.

#### **3.1 Apparatus**

The equipment utilized throughout the entire experiment is listed below.

- Hot Plate
- Digital Weight Balance
- Centrifuge
- Micro Pipette
- Separation Funnel
- Amicon centrifuge filter
- Centrifuge Tubes
- Microwave Oven
- Rotary Evaporator

##### *Hot Plate*

Hot plate has an inbuilt electric heating source that is used to heat the sample. It also has a magnetic stirring machine that uses a magnetic bar to stir the sample.

##### *Digital Weight Balance*

In laboratories, a digital weight balance is employed to precisely measure the sample. In our lab, we employed a weight balance with a minimum count of 0.01 mg.

##### *Centrifuge*

A centrifuge works based on the sedimentation principle, whereby materials are separated according to their densities under the effect of gravity. During centrifugation, lighter particles remain at the top while heavier particles settle to the bottom. For our experiment we use HERMAL 50 ml centrifuge and 15 ml centrifuge machine.

### *Micro Pipettes*

Micro pipettes are used to measure extremely small amounts of liquid, specifically in micro liters. For our measurements, we employ a 10 to 100 ul pipette and a 100 to 1000 ul pipette.

### *Separation Funnel*

Immiscible liquids are separated using a separation funnel. Two layers appear in a separatory funnel when two immiscible liquids are added. The lower layer will be composed of denser solvents.

### *Amicon centrifuge filter*

Amicon Centrifuge filter uses pressurized ultrafiltration at high flow rates to concentrate the sample. Samples contain gold nanoparticles of very small size, so we use these filters to concentrate the sample.

### *Centrifuge Tubes*

Liquids are contained in centrifuge tubes. Centrifugation is a process that splits a sample into its component parts by quickly rotating it around a fixed axis. It has conical bottoms which help to collect any solid or denser particles.

### *Microwave Oven*

Microwave Oven use radiation to heat the sample. We use it to heat the agarose for the preparation of gel.

### *Rotary Evaporator*

A rotary evaporator, also known as a rotavap, is a tool used in chemical laboratories to remove solvents effectively and delicately from samples. Rotary Evaporator removes the solvent by evaporating it under reduced pressure. This reduced pressure helps the solvent to boil at a lower temperature than its normal boiling temperature. This is also used for coating on the surface of nanoparticles.

### ***3.2 Characterization Technique***

The following characterization techniques are used to analysis the sample and the effect of sample on Cancer Cell.

- X-ray Diffraction (XRD)
- Fourier-transform infrared spectroscopy (FTIR)
- Raman spectroscopy
- UV-Vis spectroscopy
- Gel electrophoresis
- Zeta Potential
- Antioxidant
- Cytotoxicity assays

#### ***X-ray Diffraction (XRD)***

X-ray diffraction is a nondestructive method that can provide a comprehensive examination of a substance's chemical makeup, physical characteristics, and crystallographic structure. X-ray diffraction works on the principle of constructive interference between monochromatic light and crystalline structure. There is constructive interference between sample and incident light when it satisfies Braggs law.

$$n\lambda = 2d\sin\theta$$

The wavelength of electromagnetic radiation is related to the diffraction angle and lattice spacing in a crystalline sample by means of this law. These diffracted X-rays are then located, scrutinized, and tallied. Since each material has a distinct set of d-spacings, the conversion of the diffraction peaks to d-spacings enables the identification of a substance. This is typically accomplished by contrasting the d-spacings with recognized reference patterns.

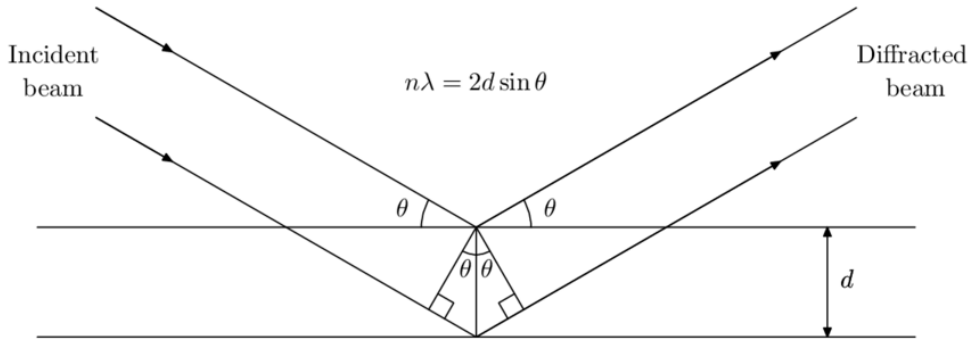


Figure 11: Braggs Law. [42]

The three essential parts of an X-ray diffractometer. X-ray tube, a sample holder, and an X-ray detector. X-rays are produced when heat is provided to the filament in cathode ray tube to produce electrons. Then voltage is provided to accelerate the electron towards the target. These electrons strike with target. Characteristic X-ray spectrum arise when electrons have sufficient energy to knock inner shell electrons out of the target material. Most of the XRD analysis source is Cu and  $k\alpha$  segment is separated for diffraction analysis.

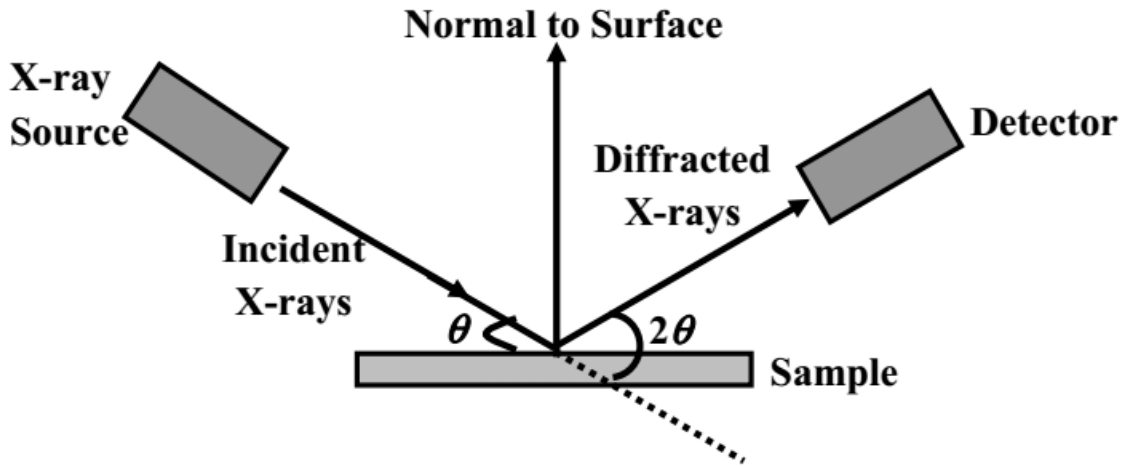


Figure 12: Working Principle of X-Ray Diffraction [43].

These X-rays are converged and targeted at the sample. Rotating the sample and detector allows for the measurement of the reflected X-rays' intensity. An intensity peak appears, and constructive interference occurs when the incident X-rays' geometry satisfies the conditions of the Bragg Equation. A detector not only collects but also processes this X-ray radiation. After being transformed into a count rate, the signal is then transmitted to a device, such as a computer monitor or printer.

### *Fourier-transform infrared spectroscopy (FTIR)*

FTIR is a type of infrared spectroscopy. Different molecules have different structures. When radiation pass through them, they produce different spectra. FTIR works on this principle when a sample is exposed to radiation. A portion of the radiation travels through the sample and is absorbed by it. This passing radiation is detected by FTIR to produce spectra. This spectrum is used to identify and distinguish molecules.

These benefits of Fourier transform infrared (FTIR) arise from its conjunction with an interferometer, which acts as an infrared light "source" and facilitates faster processing. An algorithmic procedure called the Fourier transform analyses waves to determine their frequency in respect to time. We use a graph known as an "interferogram" as the "output" of the interferometer, rather than the spectroscopic spectrum. The Fourier transform of the interferogram yields the familiar and useful spectrum graph for infrared spectroscopy.

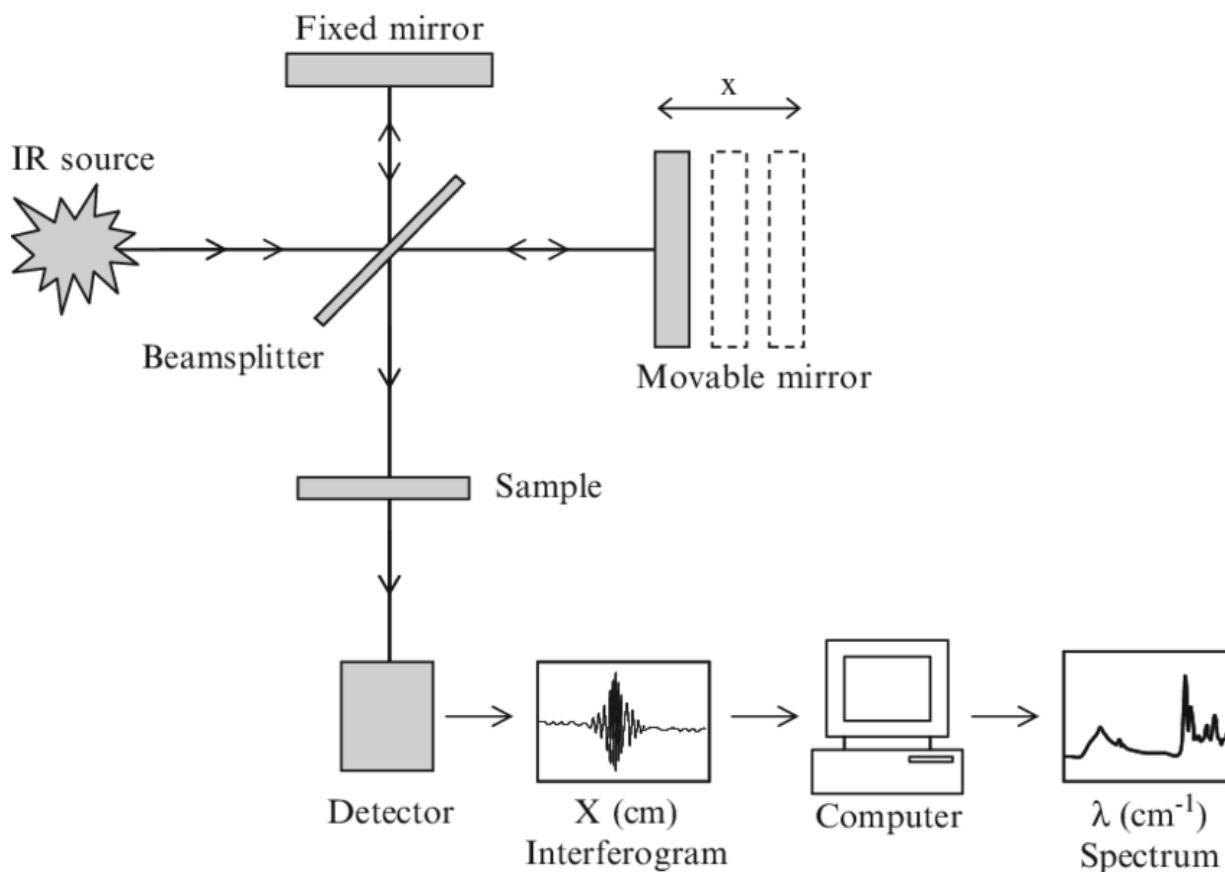


Figure 13: Schematic Diagram of Fourier-transform Infrared spectroscopy (FTIR) [44].



Particularly, radiation with a particular wavelength will be absorbed by covalent bonds in molecules, altering the vibrational energy of the bond. The type of vibration that the infrared light causes (bending or stretching) depends on the atoms in the link. The varied frequencies that various bonds and functional groups absorb cause variations in the transmittance spectrum for different molecules.

There are numerous explanations for why FTIR is the most used approach for infrared spectroscopy. To begin with, there is no damage to the sample. The second advantage is that it works much faster than previous techniques. Thirdly, it is much more sensitive and precise.

### ***Raman Spectroscopy***

One non-invasive method of chemical evaluation is Raman spectroscopy that offers comprehensive information on the phase and chemical composition and polymorphic, crystallinity, and molecular interactions. It is predicated on the way light and chemical reactions in a substance interact.

A molecule uses the Raman light scattering method to scatter light originating from a strong laser light source. Most of the dispersed light lacks meaningful information because it is mostly the same wavelength (or colour) as the laser's source.; this is known as Rayleigh Scatter. But a small amount of light (usually 0.0000001%) is scattered at various wavelengths (or colors) depending on the analyte's chemical makeup; this is known as Raman Scatter.

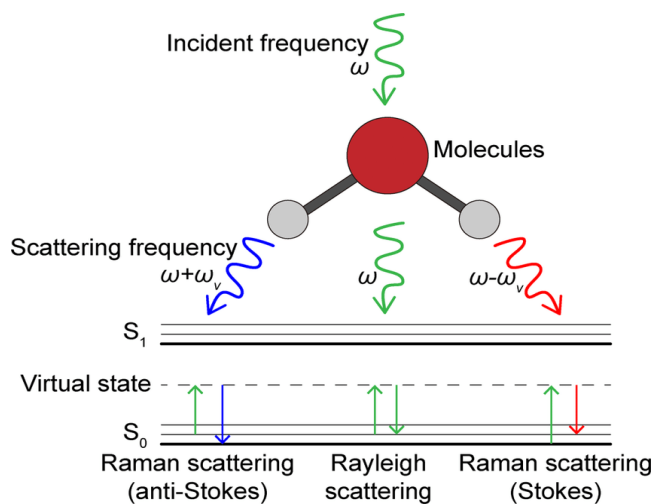


*Figure 14: Raman Scattering [45].*

Many peaks in a Raman spectrum indicate the wavelength position and strength of the dispersed Raman light. Every peak corresponds to a particular chemical bond vibration, encompassing groups of bonds such as the breathing mode of the benzene ring, chains of polymer vibrations, and lattice modes, as well as single bonds such as C-C, C=C, N-O, and C-H.

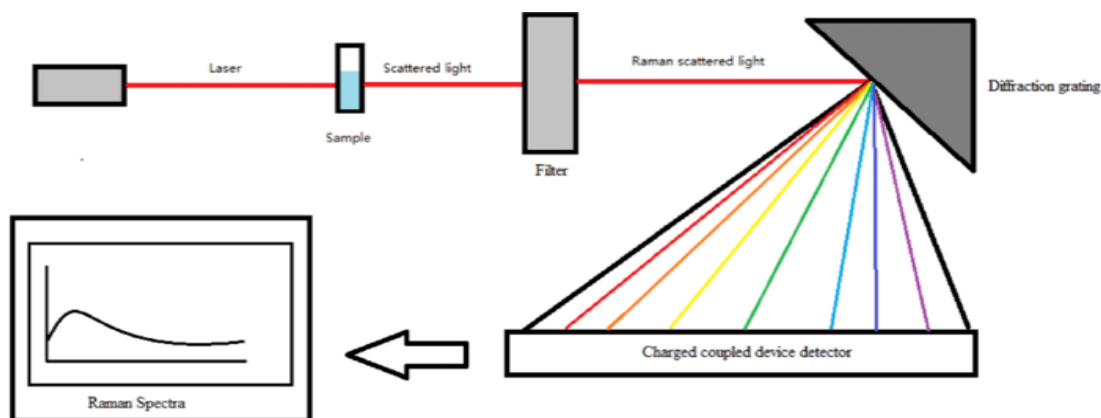


Figure 15: Schematic Diagram of Raman Spectroscopy [46].

### ***UV-Vis spectroscopy***

The analysis technique known as UV-Vis spectroscopy counts the discrete wavelengths of ultraviolet (UV) or visible light that a sample transmits or absorbs in comparison to a reference or blank sample. Because the sample composition affects this feature, it may reveal information about the contents of the sample and their concentration.

The fundamental notion behind UV-Visible Spectroscopy is that certain chemical compounds are able to absorb visible or UV rays, producing distinct spectra in the process. The interaction of matter and light is the fundamental concept of spectroscopy. A spectrum is produced by the processes of excitation and de-excitation that occur when materials absorb light. When matter absorbs UV radiation, its already-existing electrons become energized. Their change from an excited state, which has a comparably high energy associated with it, to a ground state, which is associated with a relatively low energy. An electron's absorption of UV or visible light is always equal to the variation in energy between the substance's excited and ground states.

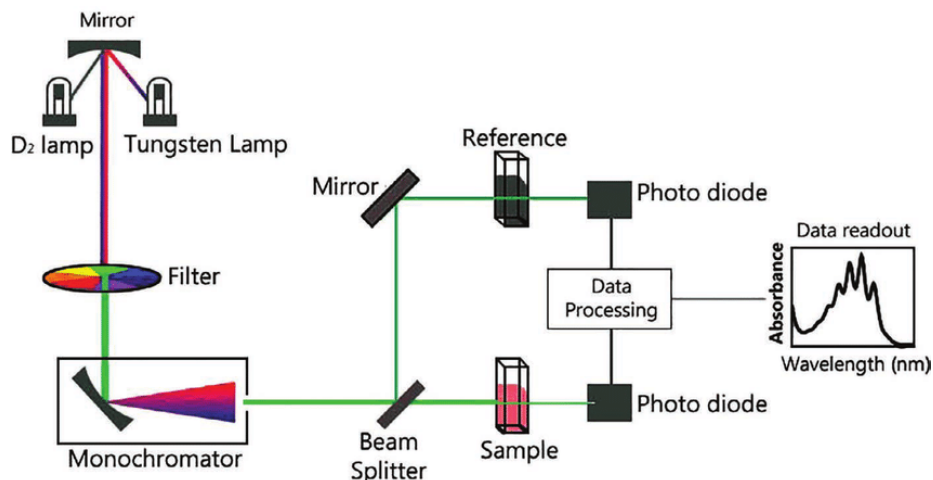


Figure 16: Schematic Diagram of UV-Vis Spectroscopy [47].

We can calculate the concentration of samples by using Beer-Lambert Law.

$$A = \epsilon dc$$

A = Absorbance

$\epsilon$  = Extinction coefficient

d = Thickness

c = Concentration

The Beer-Lambert law states that when a monochromatic light source is incident on a mixture having a material within that absorbs monochromatic light, how quickly the level of intensity of the source drops along the mixture's thickness is corresponding with the substance's concentration that absorbs the monochromatic light in the mixture and is additionally precisely correlated with the intensity of the incident monochromatic light.

### ***Gel electrophoresis***

A research method for sorting protein mixtures, nanoparticles, DNA, and RNA according to molecular size and charge is gel electrophoresis. Using an electrical field, the molecules that require separation in gel electrophoresis are driven through a gel that has microscopic pores. Applying an electric field causes the gel to become positively charged on one end and negatively charged on the other.

Because they can pass through the gel's pores more readily than longer molecules, shorter molecules travel farther and faster. It's referred to as sieving. The electric field is made up of two

charges: one end is positively charged, which pulls molecules through the gel, and the other is negatively charged, which pushes molecules through it. Molecules that require sorting are added to a well in the gel material. After the electrophoresis chamber is connected to a power source, the gel is placed inside. On the gel, discrete bands are created by the different sized molecules.

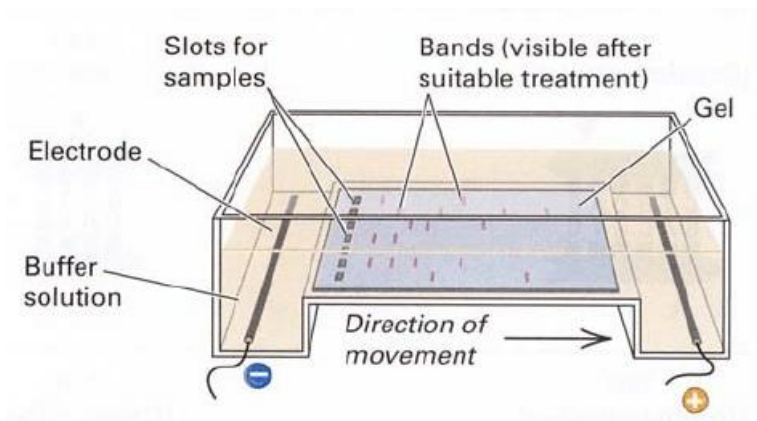


Figure 17: Apparatus used for gel electrophoresis.[48]

### ***Zeta Potential***

The electric potential at the shear plane—the line separating a particle from the surrounding fluid in a colloidal system—is known as the "zeta potential," which is an important principle in colloid science and electrochemistry.

A liquid-dispersed colloidal particle accumulates an electric charge through a variety of processes, including chemical reactions at the particle surface, ion adsorption, and ion dissociation. This electric charge's magnitude is measured by the zeta potential, which is affected by several variables including pH, ionic strength, and the chemical composition of the medium around it.

The long-term viability of colloidal dispersions is largely dependent on the zeta potential. Dispersion stability occurs when there is a large zeta potential (either negatively or positively charged), which causes particles to reject one another. Low zeta potential, on the other hand, can cause precipitation and particle aggregation.

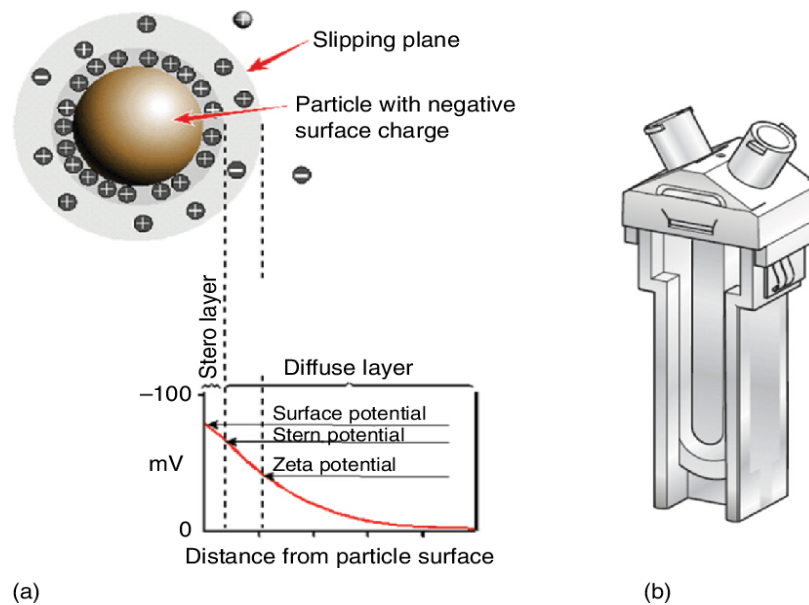


Figure 18: (a) Schematic Diagram of Zeta Potential (b) folded capillary cell. [49]

Measuring zeta potential practically offers important insights on the possibility of flocculation or particle aggregation in colloidal systems. This knowledge is crucial for several industries where colloidal stability is important, such as water treatment, food and beverage, cosmetics, and medicines.

### **Antioxidant Assay**

The DPPH (2,2-diphenyl-1-picrylhydrazyl) testing is widely used for determining the antioxidant property of compounds. DPPH is a stable free radical whose colour changes from purple to yellow when reduced. This experiment involves a molecule or antioxidant with weak A-H bonding reacting with the stable free radical DPPH• (2,2-diphenyl-1-picrylhydrazyl,  $\lambda_{\max}=517$  nm) to cause the molecule to become discolored. DPPH can be reduced by antioxidants by donating electrons; this lowers absorbance, which can be detected spectrophotometrically.

Make 0.1 mM solution of DPPH in ethanol add 0.5 ml of sample incubate it in oven at 37 C<sup>o</sup> for 40 min. Using a spectrophotometer, determine the reaction mixture's absorbance at the proper wavelength, which is often approximately 517 nm.

Calculate the Antioxidant activity by using this formula.

$$\text{Antioxidant \%} = \frac{\text{Absorbance of control} - \text{Absorbance of sample}}{\text{Absorbance of control}} \times 100$$

### *Cytotoxicity Assays*

Cytotoxicity assays evaluate a compound's ability to cause cell damage or death. Cytotoxicity assays are commonly employed in scientific studies and in drug development to test libraries for harmful chemicals. MTT assay is the most used method for determining the cytotoxicity of a dangerous substance that has been identified or created. The MTT assay distinguishes between living and dead cells.

Simply expressed, cell cytotoxicity is the ability of certain substances or mediator cells to cause the death of living cells. Using a cytotoxic agent, healthy living cells can be caused to undergo either necrosis—unintentional cell death—or apoptosis—planned cell death.

## **Chapter 4**

### **Materials and Method**

#### **Materials**

Tetrachloroauric acid (hydrogen tetrachloroaurate (III):  $\text{HAuCl}_4 \cdot x\text{H}_2\text{O}$ , 99.9 %, Alfa Aesar #12325), Tetraoctylammonium bromide  $(\text{C}_8\text{H}_{17})_4\text{NBr}$ , Toluene, Sodium borohydride ( $\text{NaBH}_4$ ), Hydrochloric Acid HCL, Sodium Hydroxide ( $\text{NaOH}$ ), Dodecanethiol ( $\text{C}_{12}\text{H}_{25}\text{SH}$ ), Methanol, Chloroform, Poly (methyl acrylate) (PMA) 60% dodecylamine, Polyethylene Glycol (PEG), (1-ethyl-3-(3-dimethylaminopropyl) carbodiimide (EDC), Boric Acid, Tris base, Ethylenediamine tetraacetic acid (EDTA), Agarose, Betulinic Acid:  $\text{C}_{30}\text{H}_{48}\text{O}_3$ , 97%, Macklin.

#### **4.2 Method**

##### **4.2.1 Synthesis of Gold Nanoparticles**

A modified two-phase (organic-aqueous) procedure was used to create Au particles with an inorganic core diameter of approximately 4 nm.

1 Solution A: Prepare stock solution of gold salt. Dissolve 1 g of tetrachloroauric acid (hydrogen tetrachloroaurate (III):  $\text{HAuCl}_4 \cdot x\text{H}_2\text{O}$ , 99.9 %, Alfa Aesar #12325) in 250ml of distilled water to make 10 Mm stock solution of Au salt. Colour of solution is clear and yellow.

2 Solution B: 2.17 g tetraoctylammonium bromide  $(\text{C}_8\text{H}_{17})_4\text{NBr}$  dissolved in 80 ml of toluene. The solution is clear and colorless.

3 In a 500 mL separating funnel, add 75ml of solutions A and add solution B in it. The mixture should be gently shaken for about five minutes, or until the toluene phase turns red and the aqueous phase loses its yellow colour. After that, the aqueous solution is discarded. The final solution is known as solution C.



*Figure 19: Synthesis of Gold Nanoparticles by Two Phase Method.*

4 Dissolve 334 mg of sodium borohydride ( $\text{NaBH}_4$ ) in 25 ml of distilled water. The color of the solution is colorless with some gas bubbles. This solution must be prepared freshly because of hydrolysis of sodium borohydride.

5 In a 250 mL round flask, pour solution C and mix it using a magnetic stirring apparatus. Immediately after that, add solution of sodium borohydride dropwise. For at least 60 minutes, keep stirring the resultant solution. The ultimate reaction mixture is termed as solution D.

6 In a clean 500 mL separating funnel, pour solution D. Then add the first 25 ml of HCl, carefully shake the mixture for 1 minute, and remove the aqueous phase. Add 25 mL of NaOH after that, shake and discard the aqueous phase again. After shaking and adding 25 mL of distilled water, the aqueous phase is discarded. The final stage should be carried out at least four more times until the aqueous phase becomes colorless. This solution is termed as solution E.

7 To get a good size dispersion by Oswald ripening, transfer solution E into a fresh 250 mL round flask and stir continuously on the magnetic stirring machine overnight. The outcome is referred to as solution F.

8 Add solution F in round flask adding 10 mL of Dodecanethiol ( $\text{C}_{12}\text{H}_{25}\text{SH}$ ) in it. Heat the mixture for 2 hours at  $65^\circ\text{C}$ . Ligand exchange takes place at this stage. Solution G is the ultimate solution.



9 Fill several 50 mL centrifuge vials with solution G and centrifuge for 5 minutes at 2000 rpm. To remove any larger particles, take the supernatant and discard the precipitate. The ultimate solution is referred to as solution S.

10 Pour 20 ml of solution S in several 50 ml of centrifuge vials. Then fill these vials with methanol. After that centrifuge it at 2000 rpm for 5 min. Collect the precipitate after dissolving it in chloroform and discard the supernatants. This step is intended to remove any tiny compounds that are present in excess, such as dodecanethiol and tetraoctylammonium bromide.

Hydrophobic dodecanethiol protected AuNPs with an average diameter of 4 nm is synthesized in chloroform.

#### ***4.2.2 Polymer Coating on the Surface of Gold Nanoparticles***

Poly (methyl acrylate) PMA is coated on the surface of gold nanoparticles by using rotary evaporator. We add the polymer solution with gold nanoparticles solution to the molar ratio of 100 monomer per nm<sup>2</sup>. Add 392.00 ul of PMA in 1000 ul of gold solution and add 3000 ul of anhydrous chloroform. After mixing this solution we immediately evaporate this solution under reduced pressure at 45°C until solution is completely dry by using rotary evaporator. After some time, a thin film is formed. This thin film is then dispersed in Sodium Borate Buffer (SBB) of pH 9. Now PMA is wrapped around the nanoparticles. After that solution is centrifuge in 15 ml Amicon centrifuge filter for 10 min at 4000 rpm to get rid of micelles and other tiny compounds. The concentration of solution is around 4 μM.

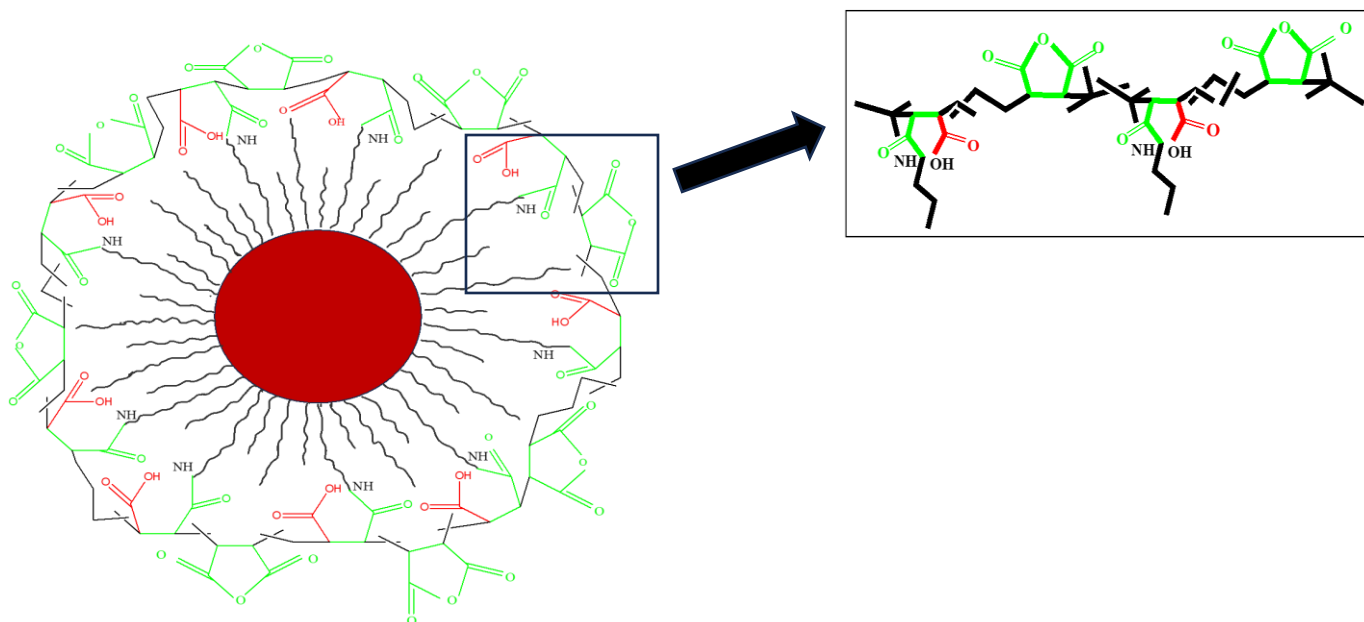
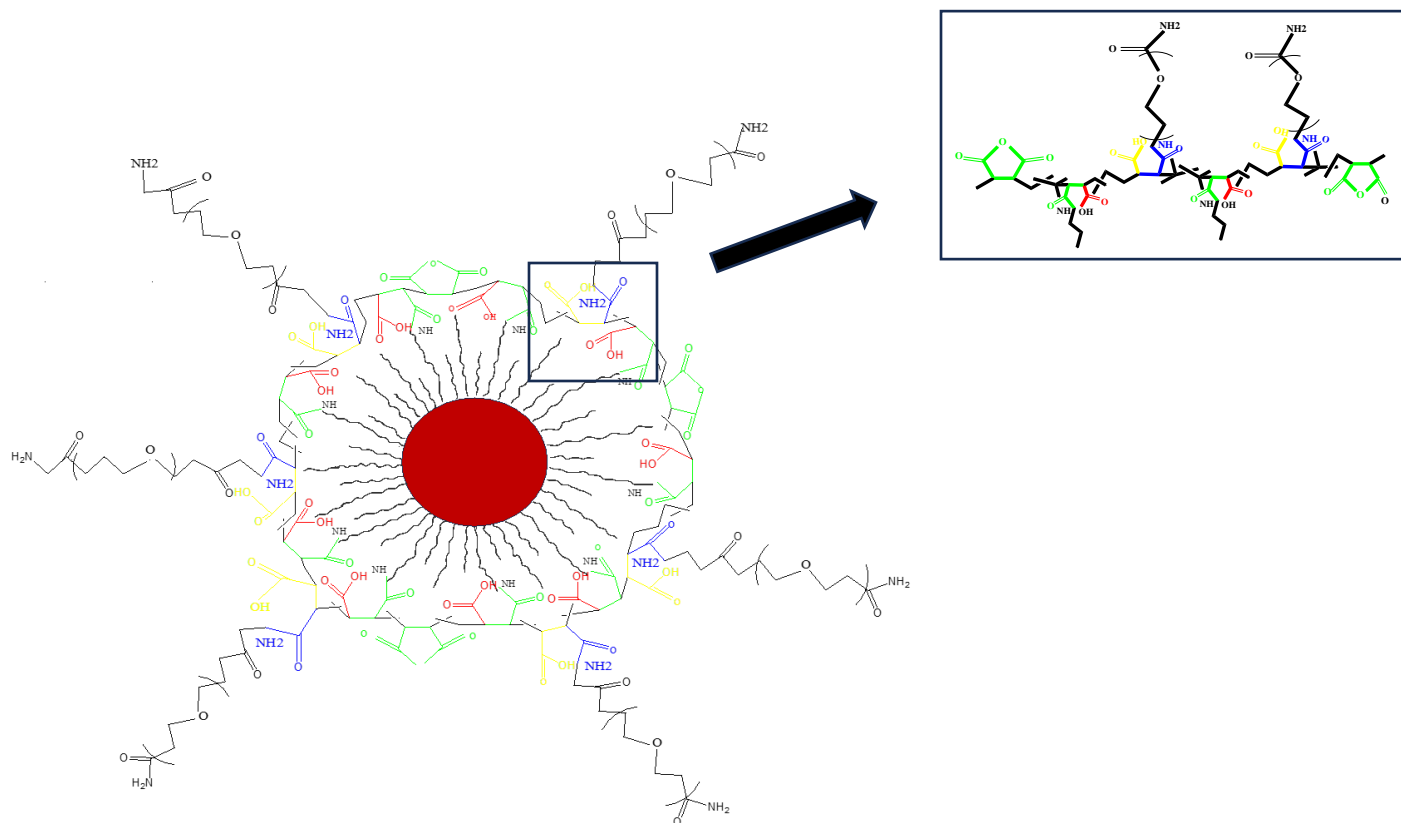


Figure 20: PMA wrapped Hydrophobic Dodecanethiol Capped Gold Nanoparticles.

#### 4.2.3 PEG Attachment to PMA Coated Gold Nanoparticles

Polyethylene Glycol (PEG) of molecular weight 2 kDa is weighed and dissolved in TBE (Tris-borate-EDTA) buffer to make stock solution of 15 Mm. Ratio is adjusted in that way that 100 diamino of PEG were added per nanoparticle. Add 1ml of gold solution into 1 ml of PEG solution then put mixture of PEG and Gold nanoparticle into refrigerator for half hour. EDC (1-ethyl-3-(3-dimethylaminopropyl) carbodiimide hydrochloride linker of concentration of 0.768 is used to link the PEG to the surface of AuNPs. 1 mg of EDC is dissolved in 1250 ul of SBB buffer. Then make different concentration of EDC from 8000 to 128000 molecules per nanoparticles. Add different concentration of EDC to the mixture of PEG and gold nanoparticles at same volume. Put these solutions in refrigerator for 2 hours. The amino terminals of the PEG are connected to the carboxyl groups on the polymer surface by the EDC. The mixtures were tested on 2% agarose gels at 100 V for an hour to determine how much PEG was present in each Au nanoparticle.



*Figure 21: PEG Modified Polymer Coated Gold Nanoparticles.*

#### **4.2.4 Drug Loaded PEG Modified Polymer Coated Gold Nanoparticles**

Betulinic Acid is a hydrophobic drug so first we dissolve it in Dimethyl sulfoxide (DMSO) and then dissolve it into TBE. Weight 8.22 mg of Betulinic Acid and dissolve it into 1.5 ml of DMSO to make 12 mM solution. Now add 333.33 ul of above solution into 666.67 ul of TBE to make 4 mM solution of drug. At the end add this solution into PEG modified polymer coated gold nanoparticle solution and leave it overnight in refrigerator. The carboxylic group of betulinic acid is attached with  $\text{-NH}_2$  group of Polyethylene Glycol (PEG).

Note Every solution should be added at the same volume.

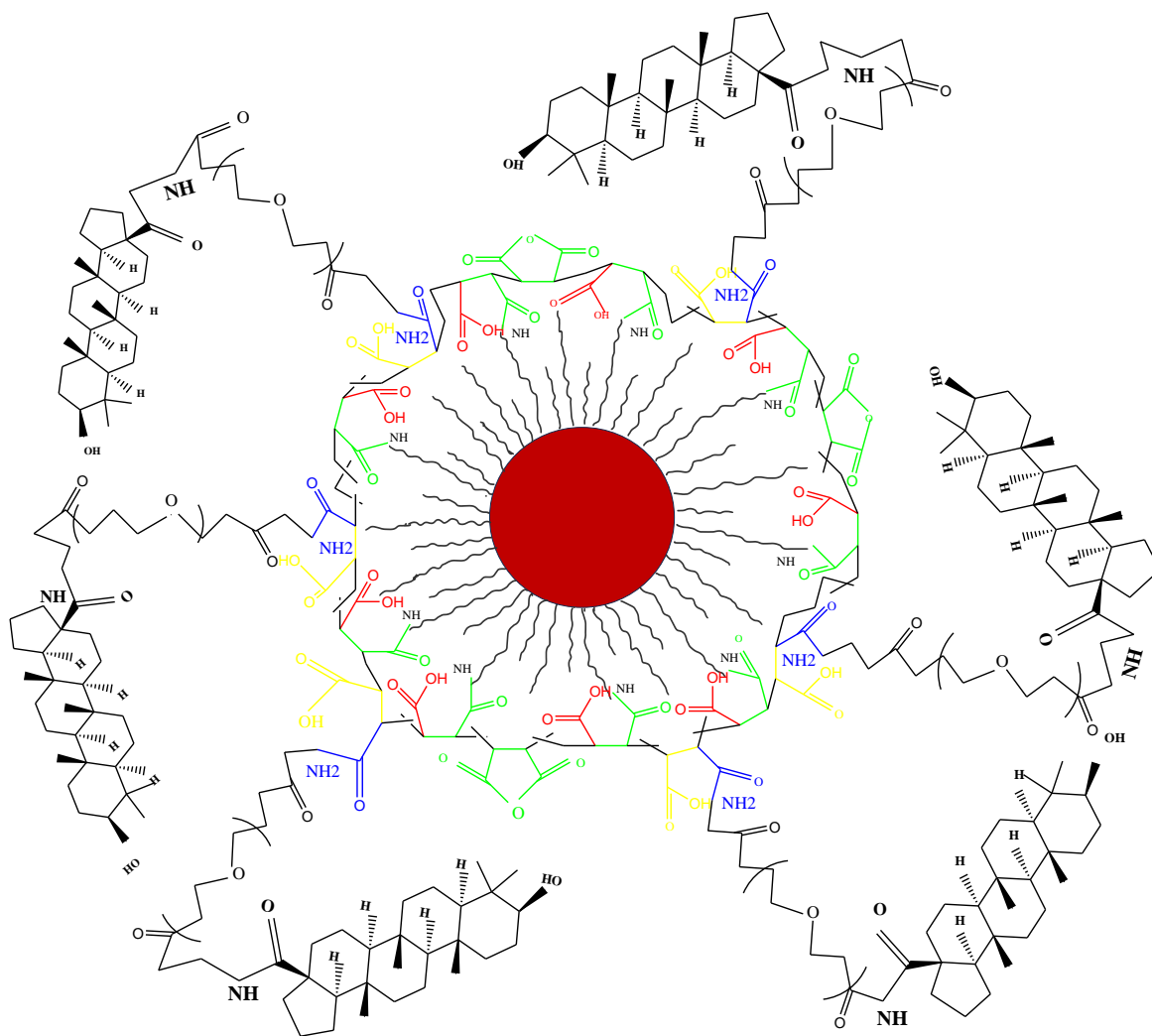


Figure 22: Drug Loaded PEG Modified Polymer Coated Gold Nanoparticles.

#### 4.2.5 Synthesis of TBE (Tris-borate-EDTA) buffer

Measure 27 g of Tris base and 13.75 g of Boric Acid Add these chemicals in 500 ml of distilled water in a beaker. Put the beaker on the sifter machine. Now weight 1.46 g of Ethylenediamine tetraacetic acid (EDTA) and add it in 10 ml of distilled water to make 0.5 M solution. Add this solution in the above solution to make 5X TBE buffer. For our experiment, we need a 1X buffer, so we add distilled water to dilute it.

#### ***4.2.6 Synthesis of Sodium Borate Buffer (SBB) of pH 9***

Weight 2.1 g of Boric Acid and 0.44 g of Sodium Hydroxide (NaOH) and add it into 500 ml of distilled water keep this on sitter machine until chemicals dissolve thoroughly to make SBB buffer of pH 9.

#### ***4.2.7 Synthesis of Agarose Gel***

Mix 1.4 g of Agarose into 70 ml of TBE buffer. Mix it well, then place the mixture in the microwave until it begins to boil. After one or two boils, transfer the mixture to the tank of the gel electro fluorescent instrument. Keep this at room temperature until the gel has hardened.

## Chapter 5

### Result and Discussion

#### UV Vis spectroscopy of Gold Nanoparticles

UV-Vis Spectra are employed to ascertain the size, concentration, and stability of nanoparticles. Gold nanoparticles show absorbance peak between 500-600 nm. Their absorbance peak based on the nanoparticles' size and form [50].

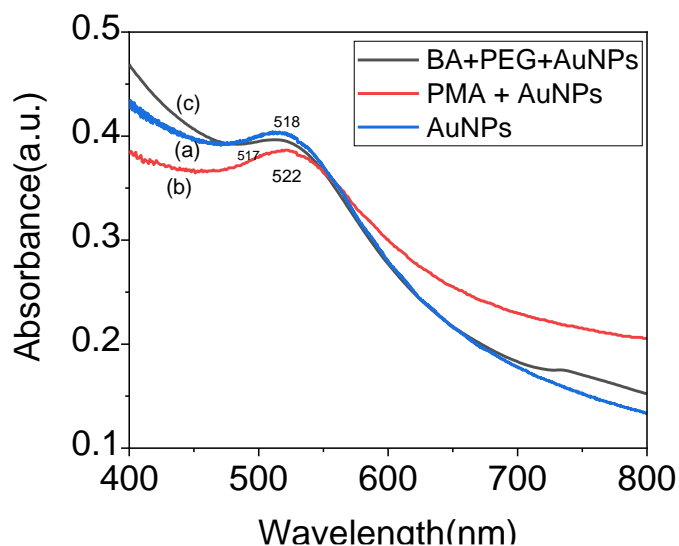


Figure 23: (a) Gold Nanoparticles; (b) Poly (methyl acrylate) (PMA) coated Gold Nanoparticle; (c) Betulinic Acid loaded Polymer coated Gold Nanoparticles.

Figure 28 (a) confirms absorbance peak caused by the production of gold nanoparticles is at 518 nm which shows that the nanoparticles are around the size of 4 nm. Surface of gold nanoparticles can be functionalized, and we can evaluate it by UV-Vis spectra (b) confirm the coating of gold nanoparticle surface with Poly (methyl acrylate) (PMA) spectrum show some red shift the local refractive index at the surface of the gold nanoparticle is changing, which is the cause of this shift. Similarly peak shift in (c) shows that Betulinic Acid is loaded on the surface of gold nanoparticle [51].

### FTIR Spectra of Gold Nanoparticles

FTIR is a type of infrared spectroscopy. Different molecules have different structures. When radiation passes through them, they produce different spectra.

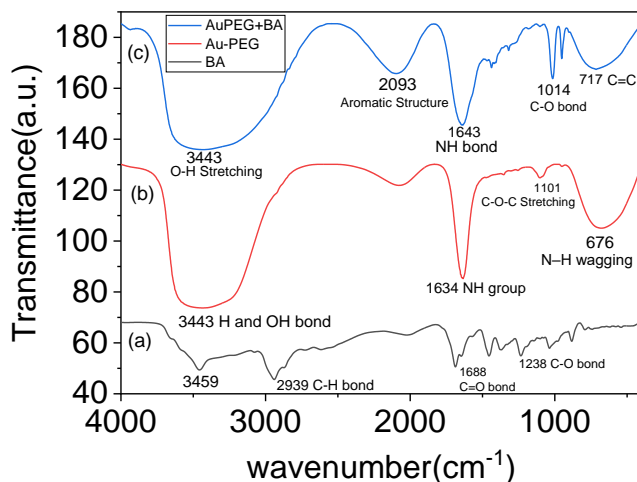
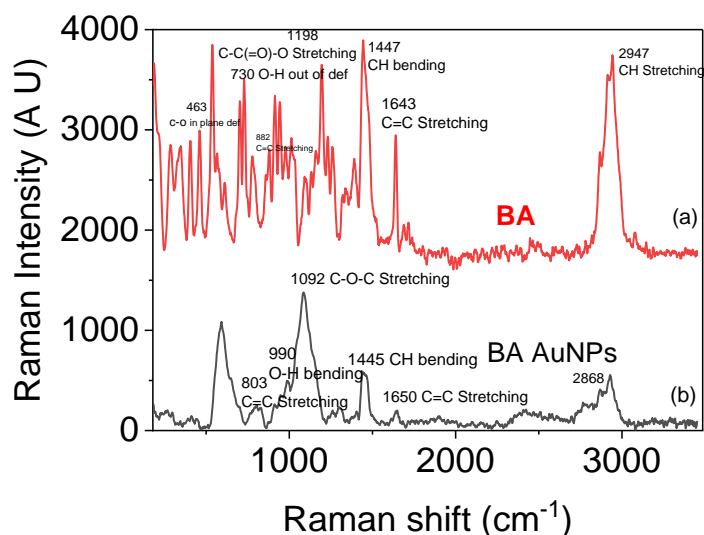


Figure 24: FTIR spectra (a) Betulinic Acid; (b) Polyethylene glycol (PEG) coated Gold Nanoparticles; (c) Betulinic Acid loaded Polymer coated Gold Nanoparticles.

Figure 29 (a) the FTIR result show peak at  $2939\text{ cm}^{-1}$  and  $2869\text{ cm}^{-1}$  confirm the presence of C-H bond. Peak at  $1688\text{ cm}^{-1}$  which reveal the presence of C=O bond and peak at  $1238\text{ cm}^{-1}$  indicate the presence of C-O bond [52]. (b) peak at  $3443\text{ cm}^{-1}$  indicates the presence of H and O-H bond. Peak at  $1634\text{ cm}^{-1}$  represents the presence of NH group.  $2069\text{ cm}^{-1}$  (N=C=S),  $1101\text{ cm}^{-1}$  (C–O–C stretching) and  $676\text{ cm}^{-1}$  (N–H wagging) confirm the presence of bound PEG [53]. (c) Peak at  $3443\text{ cm}^{-1}$  indicates the O-H stretching.  $2093\text{ cm}^{-1}$  show the aromatic structure and C-H stretching.  $1643\text{ cm}^{-1}$  peak confirms the presence of the N-H bond.  $1322\text{ cm}^{-1}$  (O-H),  $1014\text{ cm}^{-1}$  (C-O) and  $717\text{ cm}^{-1}$  (C-O bent and C=C) [54].

### ***RAMAN of Gold Nanoparticles***

One non-invasive method of chemical evaluation is Raman spectroscopy that offers comprehensive information on the phase and chemical composition and polymorphic, crystallinity, and molecular interactions. It is predicated on the way light and chemical reactions in a substance interact.



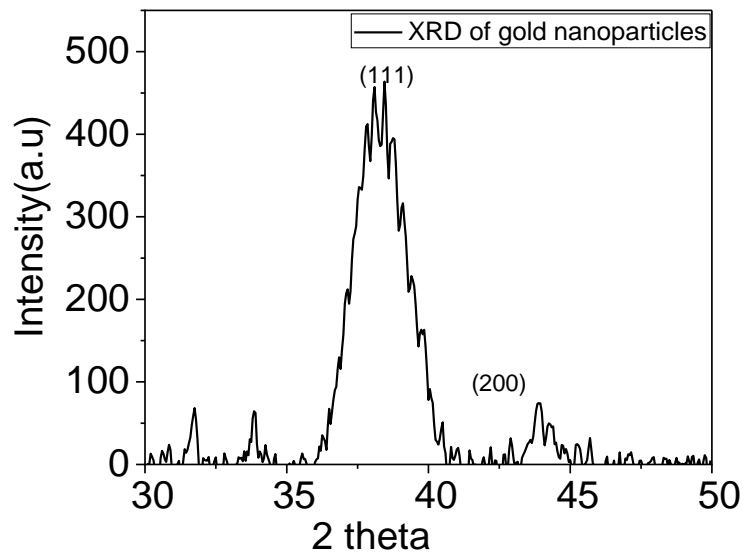
*Figure 25: (a) Raman Spectrum of Betulinic Acid (BA); (b) Raman Spectrum of Betulinic Acid loaded Polymer coated Gold Nanoparticle.*

Figure 30 (a) Raman spectrum of Betulinic Acid 2947 cm<sup>-1</sup> represents CH stretching. 1643 cm<sup>-1</sup> (C=C stretching), 1447 cm<sup>-1</sup> (C-H bending + CH<sub>2</sub> Scissoring), 1389 cm<sup>-1</sup> (C-O-H bending + CH<sub>2</sub> Wagging), 1198 cm<sup>-1</sup> (C-C(=O)-O stretching), 882 cm<sup>-1</sup> (C=C stretching), 730 cm<sup>-1</sup> (O-H out of plan def) and 463 cm<sup>-1</sup> (C-O in plan deformation). (b) Raman spectrum of Betulinic Acid loaded polymer coated gold nanoparticles 2868 cm<sup>-1</sup> is the PEG characteristic peak. 1650 cm<sup>-1</sup> indicate the C=C stretching. 1445 cm<sup>-1</sup> (C-H bending), 1306 cm<sup>-1</sup> (C-H bending), 1092 cm<sup>-1</sup> (C-O-C stretching) confirm the entrapment of Betulinic Acid in PEG coated gold nanoparticles, 990 cm<sup>-1</sup> (C-H bending + O-H bending), 803 cm<sup>-1</sup> (C=C stretching) [1, 55, 56]



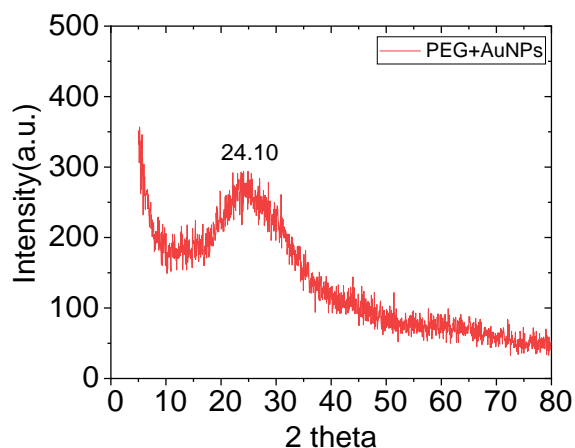
### *X-Ray Diffraction*

Figure shows the XRD pattern of gold nanoparticles synthesis by two phase method. The crystalline structure of gold nanoparticles is face center cubic fcc or icosahedral.



*Figure 26: XRD of Gold Nanoparticles.*

The diffraction peaks found at  $38.45^\circ$  (1 1 1) and  $43.95^\circ$  (2 0 0) are the same as those found for the standard gold metal (Au<sup>0</sup>) as published by the Joint Committee on Powder Diffraction Standards (JCPDS, USA). These peaks confirm the presence of crystalline gold nanoparticles. The peaks at  $31.75^\circ$  and  $33.90^\circ$  might be due to the presence of glass, impurities and noise [57].



*Figure 27: XRD of PEG Modified Polymer Coated Gold Nanoparticles.*

In figure 32 (a) represent the XRD of PEG modified polymer coated gold nanoparticles. A broad peak at  $2\theta = 24.10^\circ$  is due to the modification of gold nanoparticle surface with PEG. We get an intense peak at  $38^\circ$  for gold nanoparticles. This peak disappears in the above graph because we coat polymer on the surface. When we coat polymer on the surface it effect the crystalline structure of gold nanoparticles. [58]

### ***Gel electrophoresis***

Gel electrophoresis is used to distinguish between biomolecules and to count the quantity of polymers a molecule has bonded to its surface. We run the sample of PEG modified polymer coated gold nanoparticles and drug loaded PEG modified polymer coated gold nanoparticles on 2% agarose gels at 100 V for 1 hour to determine how many particles of PEG and Betulinic Acid attached to the surface of particles.

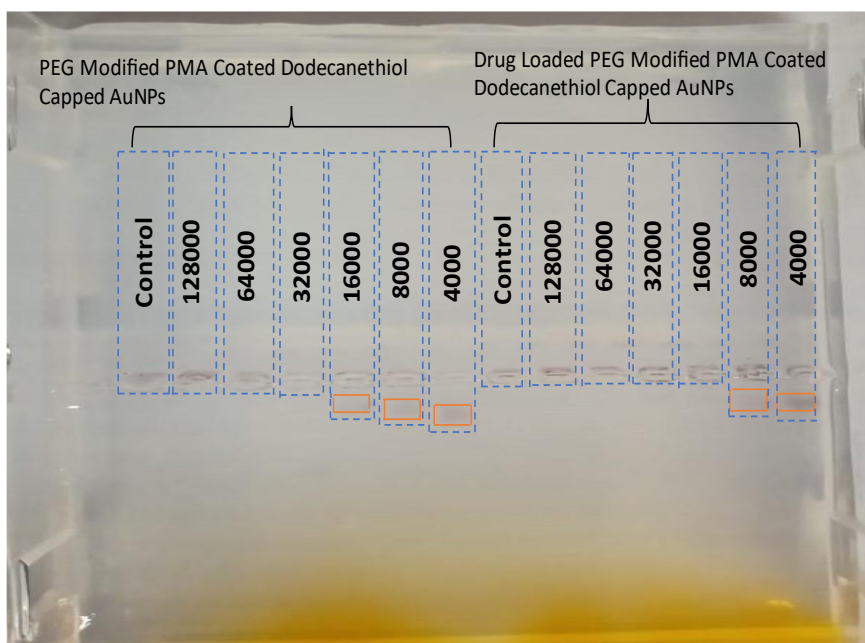


*Figure 28: Gel Electrophoresis of PEG Modified Polymer Coated Gold Nanoparticles and Betulinic Acid Loaded PEG Modified Polymer Coated Gold Nanoparticles.*

Gel electrophoresis is used to distinguish between biomolecules and to count the quantity of polymers a molecule has bonded to its surface. We run the sample of PEG modified polymer coated gold nanoparticles and drug loaded PEG modified polymer coated gold nanoparticles on 2% agarose gels at 100 V for 1 hour to determine how many particles of PEG and Betulinic Acid attached to the surface of particles. As shown in the above figure the bands retardation increases with the amount of PEG linked or drug linked to each particle. Particles with more PEG or medication attached to the surface are not released from the well. The introduction of an electric field causes Smaller molecules flow through the gel more quickly, while larger molecules move through the gel more slowly. On the gel, the variously sized molecules create discrete bands. [59]

## Zeta Potential

Zeta Potential is a crucial variable which explains the stability of colloidal suspension and charge on the surface of material. We measure the zeta potential at two different pH 5 and 10.

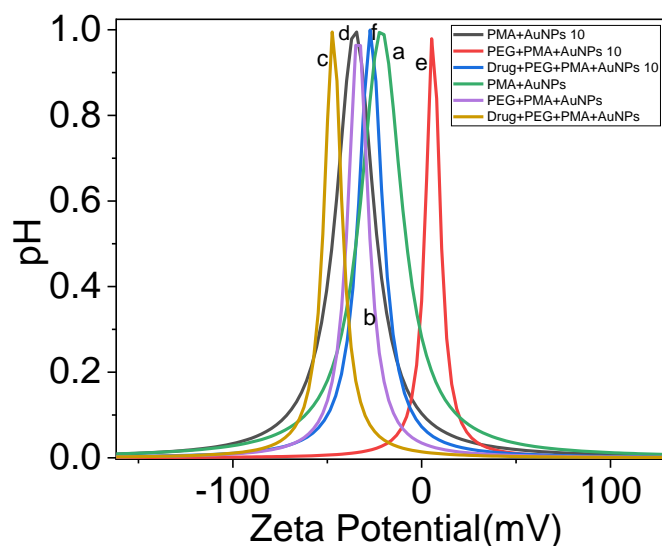


Figure 29: Zeta Potential: (a) PMA Coated Gold Nanoparticles at pH 5; (b) PEG Modified Poly (methyl acrylate) (PMA) coated Gold Nanoparticle at pH 5; (c) Betulinic Acid loaded Polymer coated Gold Nanoparticles at pH 5; (d) PMA Coated Gold Nanoparticles at pH 10; (e) PEG Modified Poly (methyl acrylate) (PMA) coated Gold Nanoparticle at pH 10; (f) Betulinic Acid loaded Polymer coated Gold Nanoparticles at pH 10.

(a) Zeta potential of unmodified gold nanoparticles at pH 5 is  $-21.35$  mV. (b) represent the zeta potential of PMA coated nanoparticles in acidic medium it is  $-33.67$  mV. This explain that the surface of particle has more negative charge because of activation of carboxyl group and suspension is stable. (c) When we attach betulinic acid to the surface of nanoparticle zeta potential is  $-46.96$  mV at pH 5 this gives information that there are more carboxyl groups present in solution and solution is highly stable. (d) represent zeta potential of unmodified gold nanoparticles in basic medium it is  $-35.37$  mV. (e) Zeta potential of modified gold nanoparticle at pH 10 is  $5.97$  mV. At pH 10 there are more Amine groups present on the surface of particle value of zeta potential is very low that explain that suspension is not stable. (f) represent the zeta potential of drug loaded nanoparticles in basic medium its value is  $-27.09$  mV that explains that there are more carboxyl groups activated on the surface.

### ANTIOXIDANT ASSAY

The DPPH was used to measure antioxidant activity. When DPPH is reduced by hydrogen or electron donation, it transforms from a purple to a yellow free radical that is stable and centered around nitrogen. The ability to carry out this reaction makes certain substances antioxidants as well as radical scavengers.[60]

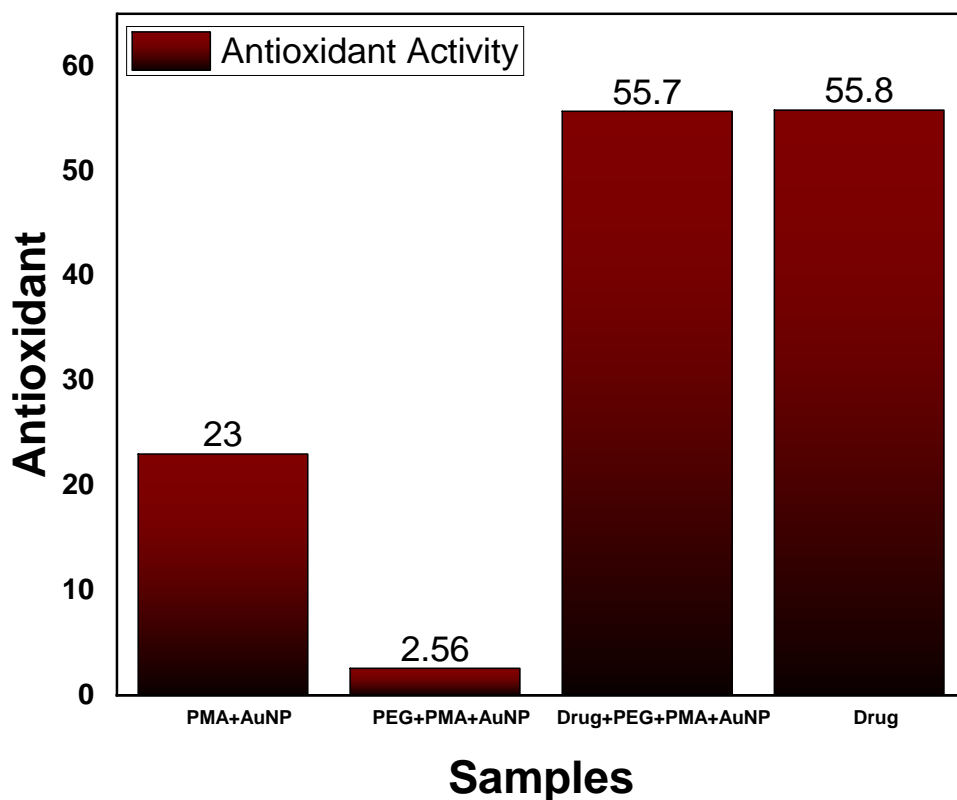


Figure 30: Antioxidant of PMA coated gold nanoparticles, PEG modified PMA coated gold nanoparticles, drug loaded gold nanoparticles and drug.

At basic pH, all the components under investigation are measured for their radical scavenging capabilities shown in Table 3. Results shows that drug show the highest antioxidant activity 55.8 %. PEG modified PMA coated AuNPs show the least antioxidant activity which is 2.56 %. It shows that when we coat polymer on the surface of nanoparticles its decreases its radical scavengers.

$$\text{Antioxidant \%} = \frac{\text{Absorbance of control} - \text{Absorbance of sample}}{\text{Absorbance of control}} \times 100$$

Table 3 Antioxidant Activity of Samples

| SR NO | SAMPLE             | ABSORBANCE OF CONTROL AT 517 NM | ABSORBANCE OF SAMPLE AT 517 NM | ANTIOXIDANT ACTIVITY % |
|-------|--------------------|---------------------------------|--------------------------------|------------------------|
| 1     | PMA + AuNPs        | 0.554875                        | 0.423973                       | 23.5 %                 |
| 2     | PEG +PMA +AuNPs    | 0.554875                        | 0.540635                       | 2.56 %                 |
| 3     | Drug+PEG+PMA+AuNPs | 1.479406                        | 0.654769                       | 55.7 %                 |
| 4     | Drug               | 1.479406                        | 0.652501                       | 55.8 %                 |

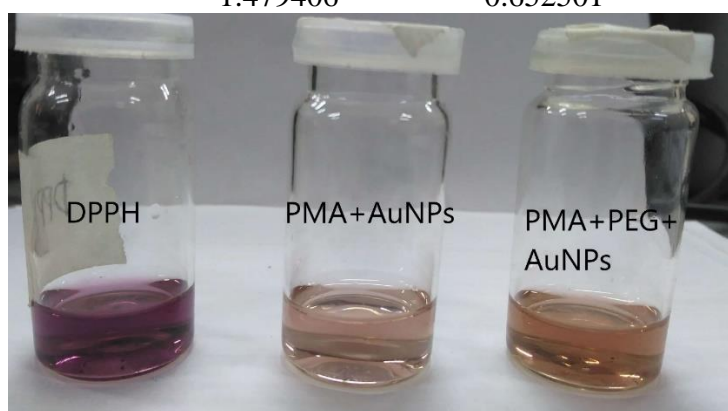


Figure 31: Image of Antioxidant of PMA AuNPs and PMA PEG AuNPs

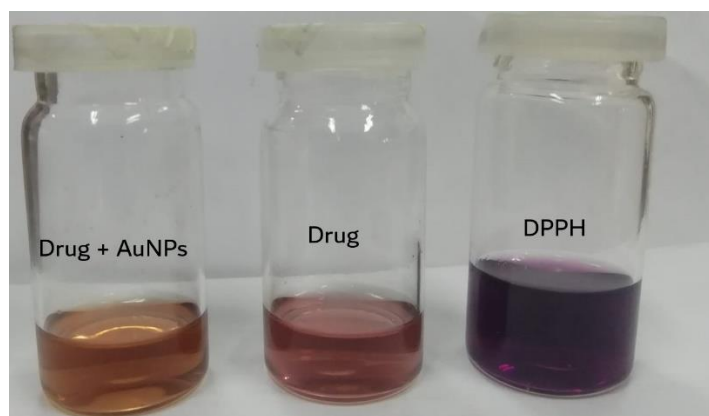
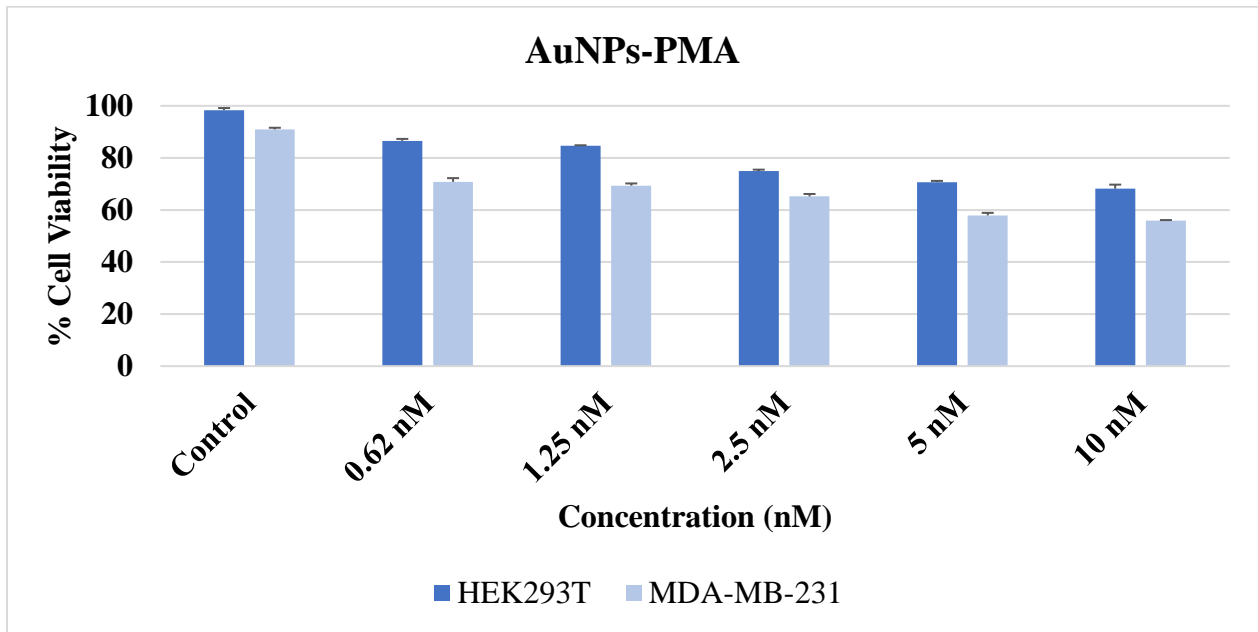


Figure 32: Image of Antioxidant of Drug Loaded AuNPs and Drug

### *Cytotoxicity*

HEK293 (ATCC CRL-1573) are human embryonic kidney cells and MDA-MB-231 (ATCC HTB-26) are invasive ductal carcinoma breast cells. HEK293 cells are widely used for research purposes like molecular biology and protein expression studies [61] [62] while MDA-MB-231 is triple-negative breast cancer cell line having lack of estrogen receptor (ER), progesterone receptor (PR) and human epidermal growth factor receptor-2 (HER2) .[63]



*Figure 33: Cytotoxicity Assessment on HEK 293T and MDA-MB-231 Cells by AUNPs-PMA.*

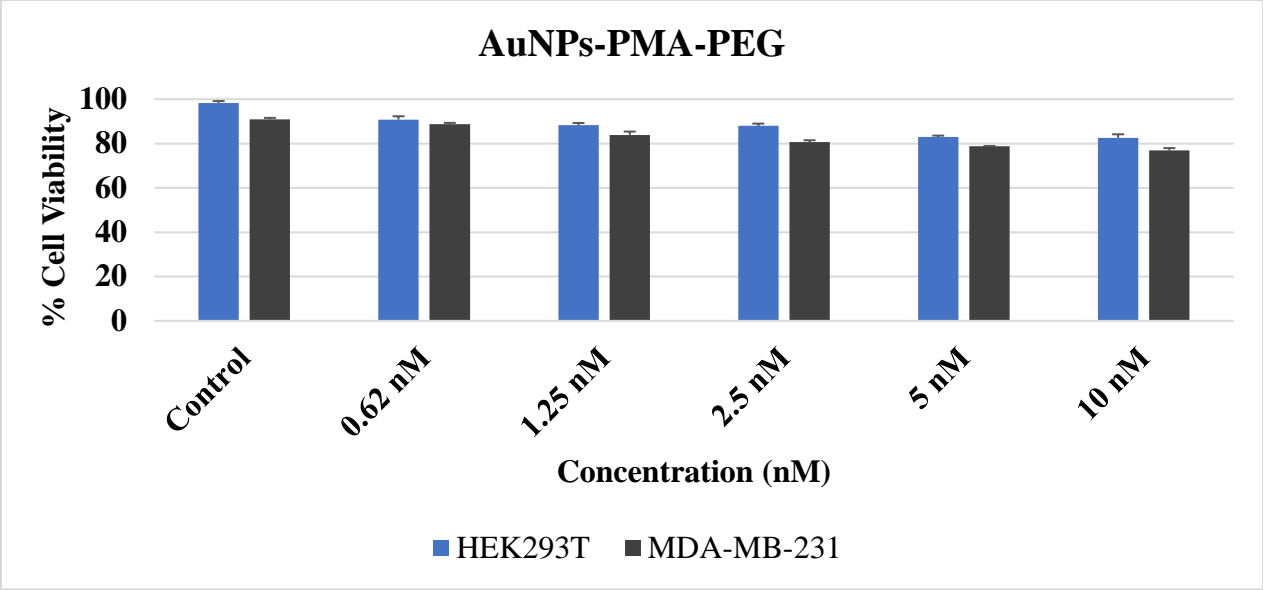


Figure 34: Cytotoxicity Assessment on HEK 293T and MDA-MB-231 Cells by AUNPs-PMA-PEG.

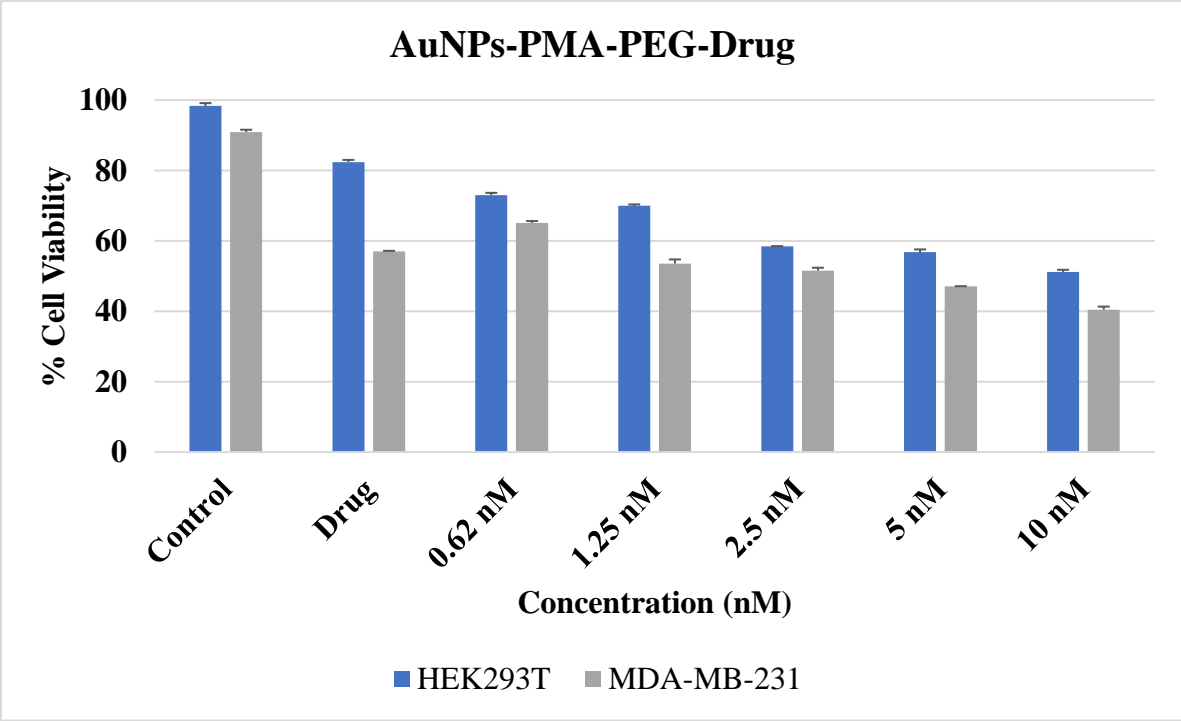


Figure 35: Cytotoxicity Assessment on HEK 293T and MDA-MB-231 Cells by AUNPs-PMA-PEG.



PMA-coated AuNPs and PMA-PEG coated AuNPs shows somewhat significant (p-value~0.0013 and 0.0028 (P <0.01\*\*)) decrease in cell viability on MDA-MB-231 over HEK293 cell lines, at 10nM and 20nM concentrations, respectively. While comparing PMA and PMA-PEG coated AuNPs cell viability, PMA coated AuNPs have significantly (p-value ~0.0156 (P <0.05\*)) decreases viability than PMA-PEG coated AuNPs at 10 nM and 20nM concentration for 72hr. This shows that AuNPs show more cytotoxicity on MDA-MB-231 cells than HEK-293 cells while PMA-PEG coated AuNPs show lesser cytotoxicity than PMA coated AuNPs and are safer to use as a drug carrier (Figure 1B). Drug conjugated AuNPs show greater cytotoxicity compared to Drug (mention Molarity) with P<0.01\*\* ( i.e., 0.0019) at 20 nM concentration for 72hr. this indicated that AuNPs as a safer carrier increases the bioavailability of drug inside the cells compared to drug (Figure 1B).

**Materials.** 3-(4,5-dimethyl-2-thiazolyl)-2,5-diphenyl-2H-tetrazolium bromide (MTT) were purchased from Sigma-Aldrich, USA. Solvents such as phosphate buffer saline, ethanol(99%), DMEM media, penicillin–streptomycin (10,000 U/mL), and fetal bovine serum (FBS) were purchased from Fisher Scientific, UK.

**Methodology.** HEK293T (ATCC CRL-1573) and MDA-MB-231 (ATCC HTB-26) cells were cultivated in DMEM supplemented with 1% of penicillin–streptomycin and 10% FBS. For MTT Assay, Cells were incubated at 37 °C under 95% moisturized air with 5% CO<sub>2</sub>. Before the experiment, cells were trypsinized (0.25% Trypsin and EDTA) and seeded (1 ×10<sup>4</sup> cells/well) (counted using eq1 & 2) on 96-well plates. The cells were incubated with PMA coated AuNPs, PEG-PMA coated AuNPs, and drugs conjugated PEG-PMA coated AuNPs for 72hr to analyze cell viability using 10µl (5 mg/mL) MTT solution (3-4 hr incubation) followed by the addition of 100 µl DMSO to dissolve formazan crystals for recording absorbance in microplate reader at 570nm. [64, 65] For MTT assay results evaluation following formula was used (eq 3):

### Equation 1

**Media required for plating**

$$= \left( \text{number of squares counted} \times \frac{1 \times 10^4 \text{ cells}}{\text{ml}} \right) \div \text{Total counted cells}$$

### Equation 2

$$C_1V_1 = C_2V_2$$

**Equation 3**

$$\% \text{ Cell viability} = \frac{(\text{Sample Absorbance} - \text{Blank Absorbance})}{(\text{Control Absorbance} - \text{Blank Absorbance})} * 100$$

## *Conclusion*

In this study, I have effectively produced gold nanoparticles measuring approximately 4 nm in diameter. The surface modification of these nanoparticles was achieved using the polymer Polyethylene Glycol (PEG), and successful loading of the nanoparticles with the hydrophobic drug Betulinic Acid was accomplished. Surface modification and successful linkage of drug to particle surface is confirmed by different characterization techniques like UV, FTIR, Raman Spectroscopy and XRD. Surface Charge was determined by Zeta Potential. The number of Polymers and particles of drug attach to particle surface is determined by using gel electrophoresis.

MTT Assay was performed on MDA-MB-231 cells breast cancer cells and HEK-293 normal kidney cells. PMA coated AuNPs, PEG modified PMA coated AuNPs, Drug loaded PEG modified PMA coated AuNPs and Drug was used to analysis the effect on cell viability. It was observed that PMA coated AuNPs are more toxic than PEG modified PMA coated AuNPs. Drug loaded AuNPs show highest toxicity on cell lines. It was also observed that binding of drug to AuNPs increases the efficiency of drug by increasing the accumulation of reactive oxygen species (ROS).

## *Future Recommendations*

An animal model can be crafted specifically for in vivo research studies. Nanoparticles tend to accumulate in organs like lungs, brain, heart, and liver, contributing to weight fluctuation. Due to their non-degradable nature, nanoparticles persist within cells, posing potential health concerns. Limited and inconsistent data exists regarding the toxic effects of metallic nanoparticles in vivo studies. An animal model is useful for solving these problems.

Polyethylene Glycol (PEG) coated Gold Nanoparticles (AuNPs) exhibit low cytotoxicity and enhanced stability in culture mediums. Different PEG of different lengths can also be used for surface modification for detailed studies.

The release of cytochrome C can be identified through Western blotting. This study is very useful for the study of mitochondrial apoptosis pathway. Further studies can be conducted on different cancer cell lines for better understanding of Betulinic Acid Coated gold nanoparticles.

Despite their advantages, PEG-coated nanoparticles can trigger acute inflammation and induce apoptosis in normal liver cells. The distribution pattern of nanoparticles in various organs raises concerns about their long-term impact on health. The persistent presence of non-degradable nanoparticles within cells may have physiological consequences. Metallic nanoparticles' toxic activities lack comprehensive and standardized assessment across different studies. PEG modification of AuNPs enhances biocompatibility but may elicit undesirable effects in specific cell types. Understanding the nuanced interactions of nanoparticles in biological systems is crucial for assessing their overall safety.

## References

- [1] S. Boca, D. Rugina, A. Pinte, N. Leopold, and S. J. J. o. N. Astilean, "Designing gold nanoparticle-ensembles as surface enhanced Raman scattering tags inside human retinal cells," vol. 2012, 2012.
- [2] A. Rauniyar *et al.*, "Federated Learning for Medical Applications: A Taxonomy, Current Trends, and Research Challenges," p. arXiv: 2208.03392, 2022.
- [3] N. K. J. J. o. P. Maurya and Phytochemistry, "Nutrients in diet that effective in cancer prevention," vol. 8, no. 2, pp. 2296-2304, 2019.
- [4] R. A. J. S. A. Weinberg, "How cancer arises," vol. 275, no. 3, pp. 62-70, 1996.
- [5] Y.-S. Sun *et al.*, "Risk factors and preventions of breast cancer," vol. 13, no. 11, p. 1387, 2017.
- [6] G. N. Sharma, R. Dave, J. Sanadya, P. Sharma, K. J. J. o. a. p. t. Sharma, and research, "Various types and management of breast cancer: an overview," vol. 1, no. 2, p. 109, 2010.
- [7] D. T. Debela *et al.*, "New approaches and procedures for cancer treatment: Current perspectives," (in eng), *SAGE Open Med*, vol. 9, p. 20503121211034366, 2021.
- [8] H. Yildizhan *et al.*, "Treatment strategies in cancer from past to present," in *Drug targeting and stimuli sensitive drug delivery systems*: Elsevier, 2018, pp. 1-37.
- [9] A. Tewabe, A. Abate, M. Tamrie, A. Seyfu, and E. Abdela Siraj, "Targeted Drug Delivery - From Magic Bullet to Nanomedicine: Principles, Challenges, and Future Perspectives," (in eng), *J Multidiscip Healthc*, vol. 14, pp. 1711-1724, 2021.
- [10] G. Liu *et al.*, "A Review on Drug Delivery System for Tumor Therapy," (in English), Review vol. 12, 2021-October-04 2021.
- [11] E. Ratemi, A. Sultana Shaik, A. Al Faraj, R. J. C. Halwani, and E. Allergy, "Alternative approaches for the treatment of airway diseases: focus on nanoparticle medicine," vol. 46, no. 8, pp. 1033-1042, 2016.
- [12] T. Thulasiramaraju, A. Babu, A. Arunachalam, M. Prathap, S. Srikanth, and P. J. I. J. o. B. Sivaiah, "Liposome: A novel drug delivery system," vol. 3, no. 1, pp. 5-16, 2012.
- [13] Y. Ding *et al.*, "Gold nanoparticles for nucleic acid delivery," vol. 22, no. 6, pp. 1075-1083, 2014.
- [14] S. J. Rosenthal, J. C. Chang, O. Kovtun, J. R. McBride, I. D. J. C. Tomlinson, and biology, "Biocompatible quantum dots for biological applications," vol. 18, no. 1, pp. 10-24, 2011.
- [15] A. Mahapatro and D. Singh, "Biodegradable Nanoparticles Are Excellent Vehicle for Site Directed," ed: Vivo.
- [16] M. Elsabahy, G. S. Heo, S.-M. Lim, G. Sun, and K. L. J. C. r. Wooley, "Polymeric nanostructures for imaging and therapy," vol. 115, no. 19, pp. 10967-11011, 2015.
- [17] K. Madaan, S. Kumar, N. Poonia, V. Lather, D. J. J. o. p. Pandita, and b. sciences, "Dendrimers in drug delivery and targeting: Drug-dendrimer interactions and toxicity issues," vol. 6, no. 3, p. 139, 2014.
- [18] B. Yavuz, S. B. Pehlivan, İ. Vural, and N. J. J. o. p. s. Ünlü, "In vitro/in vivo evaluation of dexamethasone—PAMAM dendrimer complexes for retinal drug delivery," vol. 104, no. 11, pp. 3814-3823, 2015.
- [19] D. L. Kirkpatrick, M. Weiss, A. Naumov, G. Bartholomeusz, R. B. Weisman, and O. J. M. Gliko, "Carbon nanotubes: solution for the therapeutic delivery of siRNA?," vol. 5, no. 2, pp. 278-301, 2012.
- [20] F.-Y. Kong, J.-W. Zhang, R.-F. Li, Z.-X. Wang, W.-J. Wang, and W. J. M. Wang, "Unique roles of gold nanoparticles in drug delivery, targeting and imaging applications," vol. 22, no. 9, p. 1445, 2017.
- [21] S. B. Yaqoob, R. Adnan, R. M. Rameez Khan, and M. J. F. i. C. Rashid, "Gold, silver, and palladium nanoparticles: a chemical tool for biomedical applications," vol. 8, p. 376, 2020.

- [22] F. B. Kamal Eddin and Y. W. J. M. Fen, "The principle of nanomaterials based surface plasmon resonance biosensors and its potential for dopamine detection," vol. 25, no. 12, p. 2769, 2020.
- [23] V. Amendola, R. Pilot, M. Frascioni, O. M. Maragò, and M. A. J. J. o. P. C. M. Iati, "Surface plasmon resonance in gold nanoparticles: a review," vol. 29, no. 20, p. 203002, 2017.
- [24] S. K. Ghosh and T. J. C. r. Pal, "Interparticle coupling effect on the surface plasmon resonance of gold nanoparticles: from theory to applications," vol. 107, no. 11, pp. 4797-4862, 2007.
- [25] G. J. A. P. Mie, "A contribution to the optics of turbid media, especially colloidal metallic suspensions," vol. 25, no. 4, pp. 377-445, 1908.
- [26] S. Link and M. A. J. T. J. o. P. C. B. El-Sayed, "Size and temperature dependence of the plasmon absorption of colloidal gold nanoparticles," vol. 103, no. 21, pp. 4212-4217, 1999.
- [27] X. Huang and M. A. J. J. o. a. r. El-Sayed, "Gold nanoparticles: Optical properties and implementations in cancer diagnosis and photothermal therapy," vol. 1, no. 1, pp. 13-28, 2010.
- [28] P. K. Jain, K. S. Lee, I. H. El-Sayed, and M. A. J. T. j. o. p. c. B. El-Sayed, "Calculated absorption and scattering properties of gold nanoparticles of different size, shape, and composition: applications in biological imaging and biomedicine," vol. 110, no. 14, pp. 7238-7248, 2006.
- [29] A. J. B. Lawen, "Apoptosis—an introduction," vol. 25, no. 9, pp. 888-896, 2003.
- [30] M. Abou-Ghali and J. J. S. j. o. b. s. Stiban, "Regulation of ceramide channel formation and disassembly: Insights on the initiation of apoptosis," vol. 22, no. 6, pp. 760-772, 2015.
- [31] M. W. Bowler, "Structural and biochemical studies of the regulation and catalytic mechanism of ATP synthase," 2005.
- [32] S. Desagher and J.-C. J. T. i. c. b. Martinou, "Mitochondria as the central control point of apoptosis," vol. 10, no. 9, pp. 369-377, 2000.
- [33] A. Yamada, R. Arakaki, M. Saito, Y. Kudo, and N. J. F. i. i. Ishimaru, "Dual role of Fas/FasL-mediated signal in peripheral immune tolerance," vol. 8, p. 403, 2017.
- [34] F. Cairrão and P. M. J. e. Domingos, "Apoptosis: molecular mechanisms," 2010.
- [35] D. R. J. C. Green, "Apoptotic pathways: ten minutes to dead," vol. 121, no. 5, pp. 671-674, 2005.
- [36] S. J. I. j. o. m. s. Fulda, "Betulinic acid for cancer treatment and prevention," vol. 9, no. 6, pp. 1096-1107, 2008.
- [37] D. A. Nedopekina *et al.*, "Mitochondria-targeted betulinic and ursolic acid derivatives: Synthesis and anticancer activity," vol. 8, no. 10, pp. 1934-1945, 2017.
- [38] S. Lu *et al.*, "Synthesis of gelatin-based dual-targeted nanoparticles of betulinic acid for antitumor therapy," vol. 3, no. 6, pp. 3518-3525, 2020.
- [39] F. Amin, D. A. Yushchenko, J. M. Montenegro, and W. J. J. C. Parak, "Integration of Organic Fluorophores in the Surface of Polymer-Coated Colloidal Nanoparticles for Sensing the Local Polarity of the Environment," vol. 13, no. 4, pp. 1030-1035, 2012.
- [40] O. Oladimeji, J. Akinyelu, A. Daniels, and M. J. I. j. o. m. s. Singh, "Modified gold nanoparticles for efficient delivery of betulinic acid to cancer cell mitochondria," vol. 22, no. 10, p. 5072, 2021.
- [41] C. A. J. Lin *et al.*, "Design of an amphiphilic polymer for nanoparticle coating and functionalization," vol. 4, no. 3, pp. 334-341, 2008.
- [42] T. J. a. p. a. Sochi, "High throughput software for powder diffraction and its application to heterogeneous catalysis," 2010.
- [43] W. W. Andualem, "GREEN SYNTHESIS OF CUO NANOPARTICLES FOR THE APPLICATION OF DYE SENSITIZED SOLAR CELL," 2020.
- [44] J. J. Ojeda, M. J. M. S. B. M. Dittrich, and Protocols, "Fourier transform infrared spectroscopy for molecular analysis of microbial cells," pp. 187-211, 2012.
- [45] L. Lin, X. Bi, Y. Gu, F. Wang, and J. J. J. o. A. P. Ye, "Surface-enhanced Raman scattering nanotags for bioimaging," vol. 129, no. 19, 2021.

- [46] Y. K. Lin, H. Y. Leong, T. C. Ling, D.-Q. Lin, and S.-J. J. C. J. o. C. E. Yao, "Raman spectroscopy as process analytical tool in downstream processing of biotechnology," vol. 30, pp. 204-211, 2021.
- [47] R. A. Soni, R. Rana, and S. Godara, "Characterization Tools and Techniques for Nanomaterials and Nanocomposites," in *Nanomaterials and Nanocomposites*: CRC Press, 2021, pp. 61-83.
- [48] S. Bengtsson, "Evaluation of transgenic *Campanula carpatica* plants," 2007.
- [49] G. Castillo, Z. Garaiova, and T. J. A. i. F. D. Hianik, "New Technologies for Nanoparticles Detection in Foods," pp. 305-341, 2017.
- [50] W. Haiss, N. T. Thanh, J. Aveyard, and D. G. J. A. c. Fernig, "Determination of size and concentration of gold nanoparticles from UV-Vis spectra," vol. 79, no. 11, pp. 4215-4221, 2007.
- [51] N. Bastús *et al.*, "The Delivery of Nanoparticles," p. 377-401, 2012.
- [52] C. O. Egbubine, M. M. Adeyemi, and J. D. J. B. o. t. N. R. C. Habila, "Isolation and characterization of betulinic acid from the stem bark of *Feretia canthioides* Hiern and its antimalarial potential," vol. 44, pp. 1-7, 2020.
- [53] J. Manson, D. Kumar, B. J. Meenan, and D. J. G. b. Dixon, "Polyethylene glycol functionalized gold nanoparticles: the influence of capping density on stability in various media," vol. 44, pp. 99-105, 2011.
- [54] A. Madhusudhan *et al.*, "Efficient pH dependent drug delivery to target cancer cells by gold nanoparticles capped with carboxymethyl chitosan," vol. 15, no. 5, pp. 8216-8234, 2014.
- [55] C. Y. Panicker, H. T. Varghese, D. J. S. A. P. A. M. Philip, and B. Spectroscopy, "FT-IR, FT-Raman and SERS spectra of vitamin C," vol. 65, no. 3-4, pp. 802-804, 2006.
- [56] C. G. Farcas *et al.*, "Thermosensitive betulinic acid-loaded magnetoliposomes: A promising antitumor potential for highly aggressive human breast adenocarcinoma cells under hyperthermic conditions," pp. 8175-8200, 2020.
- [57] S. Rajeshkumar *et al.*, "Seaweed-mediated synthesis of gold nanoparticles using *Turbinaria conoides* and its characterization," vol. 3, pp. 1-7, 2013.
- [58] M. A. Jihad, F. T. Noori, M. S. Jabir, S. Albukhaty, F. A. AlMalki, and A. A. J. M. Alyamani, "Polyethylene glycol functionalized graphene oxide nanoparticles loaded with *nigella sativa* extract: a smart antibacterial therapeutic drug delivery system," vol. 26, no. 11, p. 3067, 2021.
- [59] K. Wilson, A. Hofmann, J. M. Walker, and S. Clokie, *Wilson and Walker's principles and techniques of biochemistry and molecular biology*. Cambridge university press, 2018.
- [60] S. Medhe, P. Bansal, and M. M. J. A. N. Srivastava, "Enhanced antioxidant activity of gold nanoparticle embedded 3, 6-dihydroxyflavone: a combinational study," vol. 4, pp. 153-161, 2014.
- [61] M. Pulix, V. Lukashchuk, D. C. Smith, and A. J. J. C. o. i. b. Dickson, "Molecular characterization of HEK293 cells as emerging versatile cell factories," vol. 71, pp. 18-24, 2021.
- [62] E. Tan, C. S. H. Chin, Z. F. S. Lim, S. K. J. F. i. b. Ng, and biotechnology, "HEK293 cell line as a platform to produce recombinant proteins and viral vectors," vol. 9, p. 796991, 2021.
- [63] F. Mohammed, F. Rashid-Doubell, S. Taha, S. Cassidy, and S. J. I. j. o. o. Fredericks, "Effects of curcumin complexes on MDA-MB-231 breast cancer cell proliferation," vol. 57, no. 2, pp. 445-455, 2020.
- [64] N. A. Razak *et al.*, "Cytotoxicity of eupatorin in MCF-7 and MDA-MB-231 human breast cancer cells via cell cycle arrest, anti-angiogenesis and induction of apoptosis," vol. 9, no. 1, p. 1514, 2019.
- [65] S. Malik *et al.*, "Cytotoxicity study of gold nanoparticle synthesis using *Aloe vera*, honey, and *Gymnema sylvestre* leaf extract," vol. 8, no. 7, pp. 6325-6336, 2023.